Mechanism of catalytic cyclohydroamination by zirconium salicyloxazoline complexes

Laura E. N. Allan, Guy J Clarkson, David J. Fox, Andrew L Gott and Peter Scott**

Department of Chemistry, University of Warwick, Gibbet Hill Road, Coventry, CV7 4AL, U.K.

Email: peter.scott@warwick.ac.uk

Supporting Information

Kinetic plots

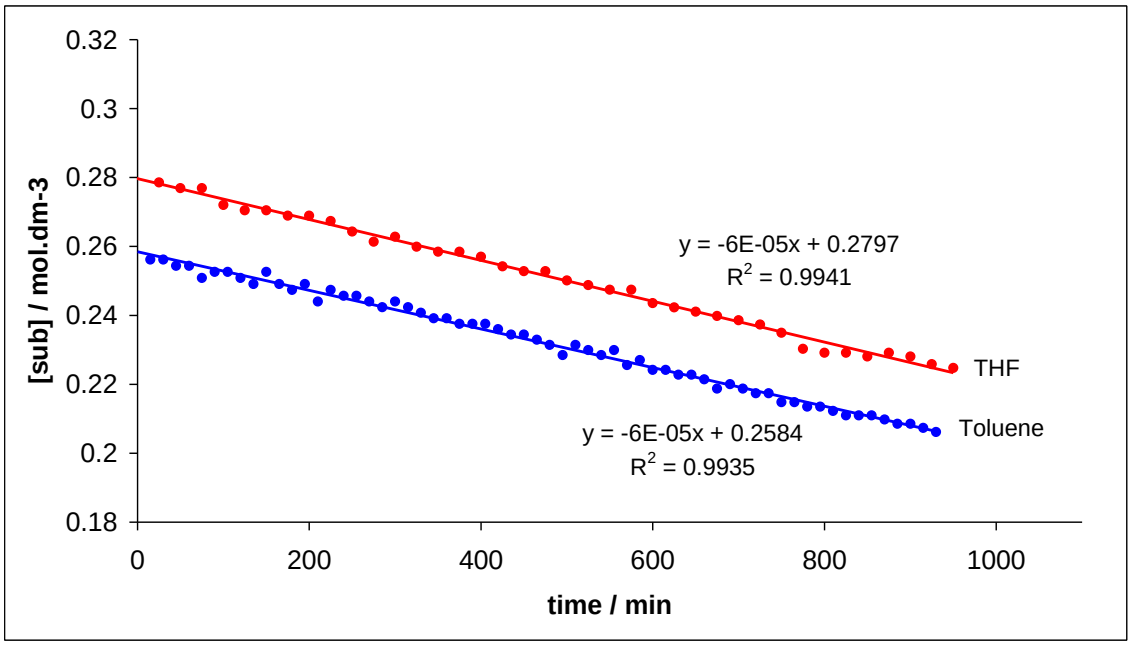

Figure S1. Kinetic plots of [substrate] versus time for hydroamination / cyclization of $H_2NCH_2CMe_2CH_2CH{=}CH_2$ at 60°C, using [Cp*Zr(NMe$_2$)$_2$(PhPhOx)] precatalyst in toluene-d$_8$ (●) and THF-d$_8$ (●).[cat]$_0$ = 0.024 M. The lines are least-squares fits to the data points.

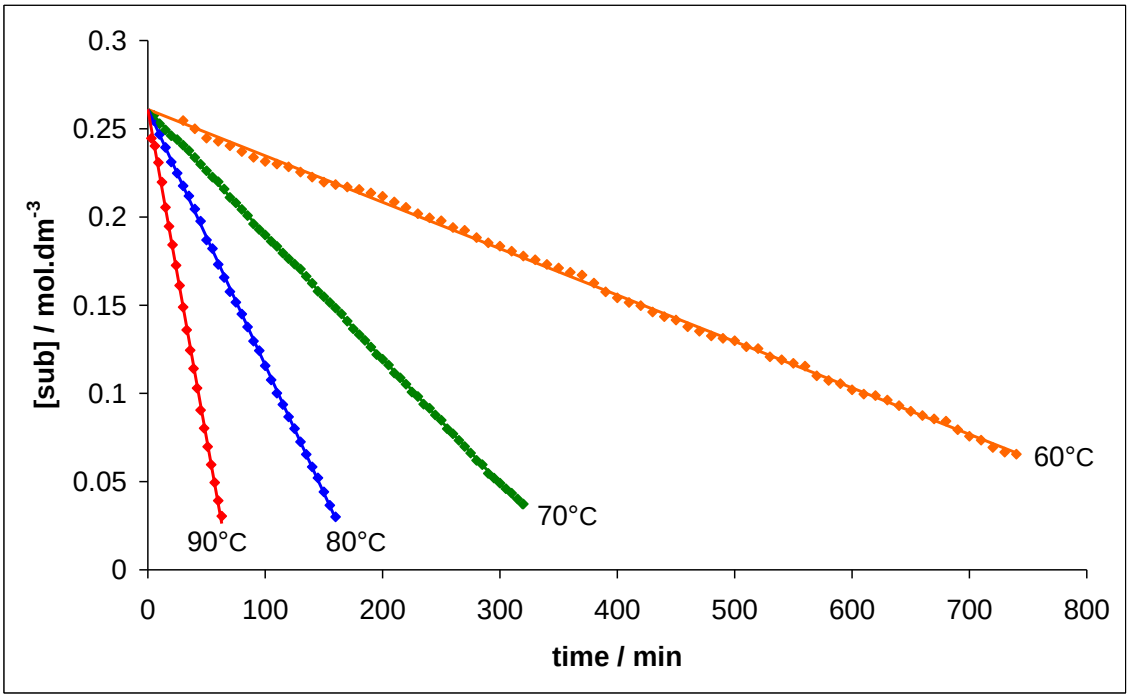

Figure S2. Kinetic plots of [substrate] versus time for hydroamination / cyclization of $H_2NCH_2CMe_2(CH_2)_2CH{=}CH_2$ as a function of temperature using $[Cp^*Zr(NMe_2)_2(PhPhOx)]$ precatalyst in toluene-d_8. The lines are least-squares fits to the data points.

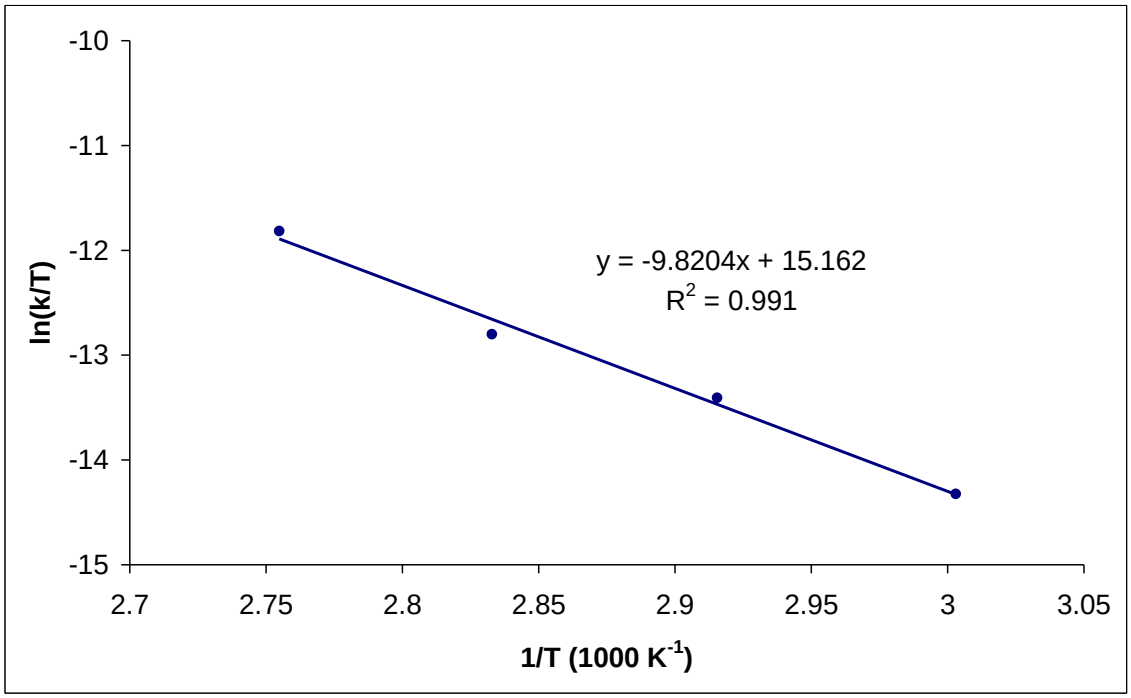

Figure S3. Eyring plot for the hydroamination / cyclization of $H_2NCH_2CMe_2(CH_2)_2CH{=}CH_2$ using $[Cp^*Zr(NMe_2)_2(PhPhOx)]$ precatalyst in toluene-d_8. The line is the least-squares fit to the data points.

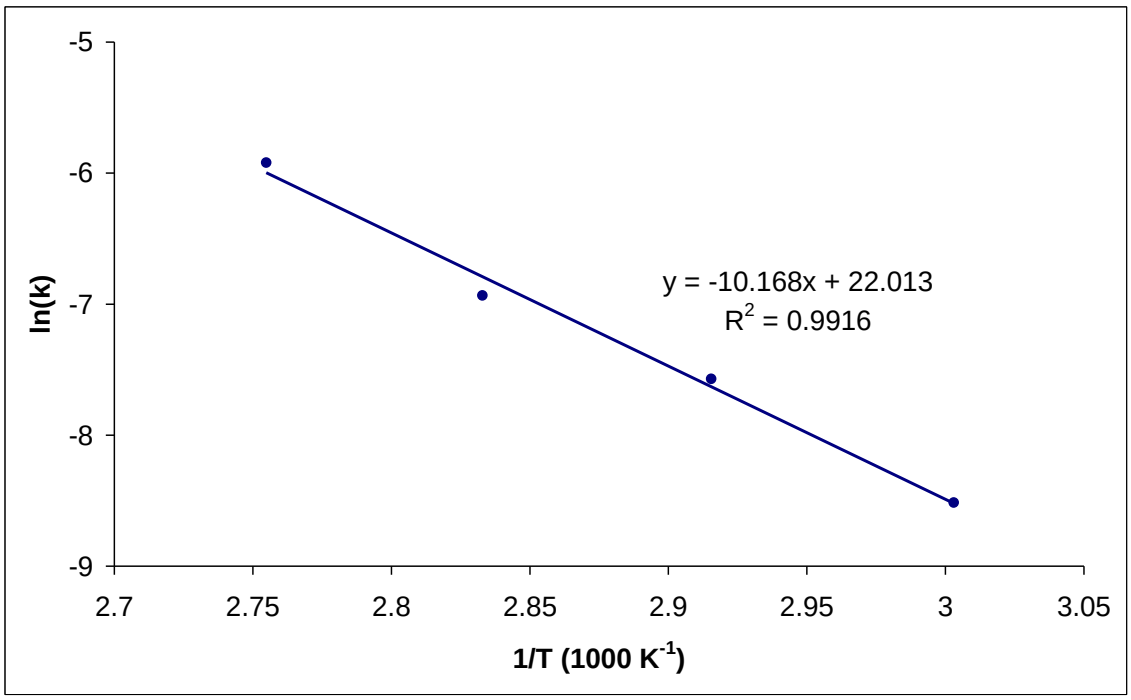

Figure S4. Arrhenius plot for the hydroamination / cyclization of $H_2NCH_2CMe_2(CH_2)_2CH{=}CH_2$ using [Cp*Zr(NMe_2)$_2$(PhPhOx)] precatalyst in toluene-d_8. The line is the least-squares fit to the data points.

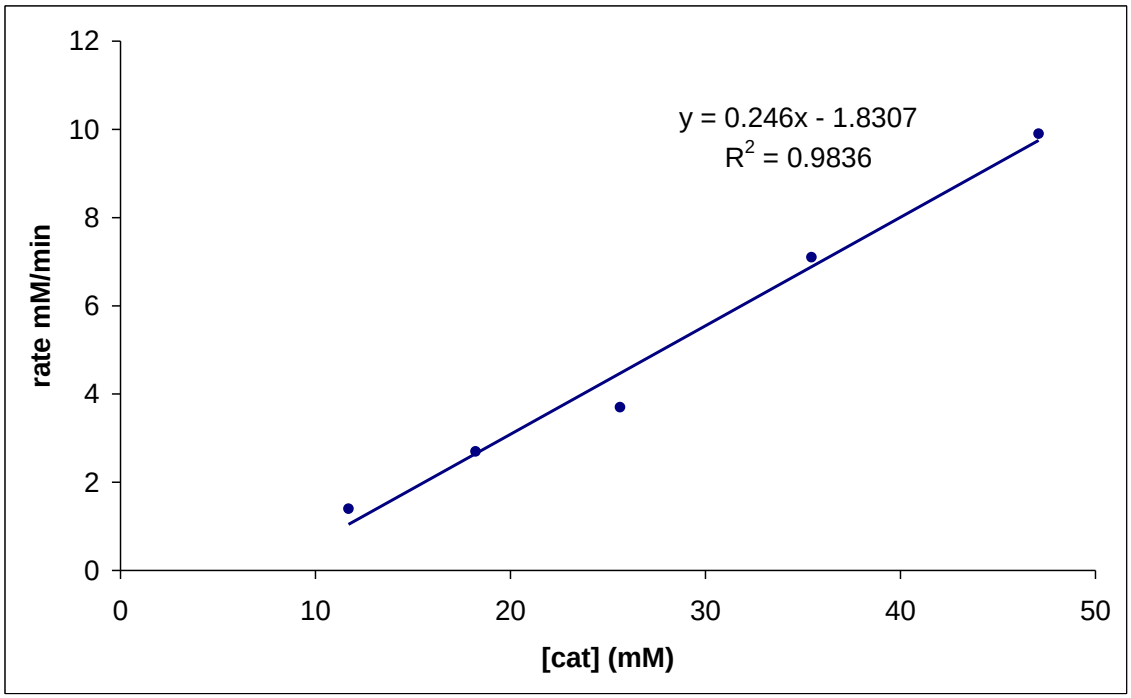

Figure S5. Determination of reaction order in zirconium concentration for the hydroamination/cyclization of $H_2NCH_2CMe_2(CH_2)_2CH{=}CH_2$ in toluene-d_8 at 90°C using the precatalyst [Cp*Zr(NMe_2)$_2$(PhPhOx)]. The line is the least-squares fit to the data points.

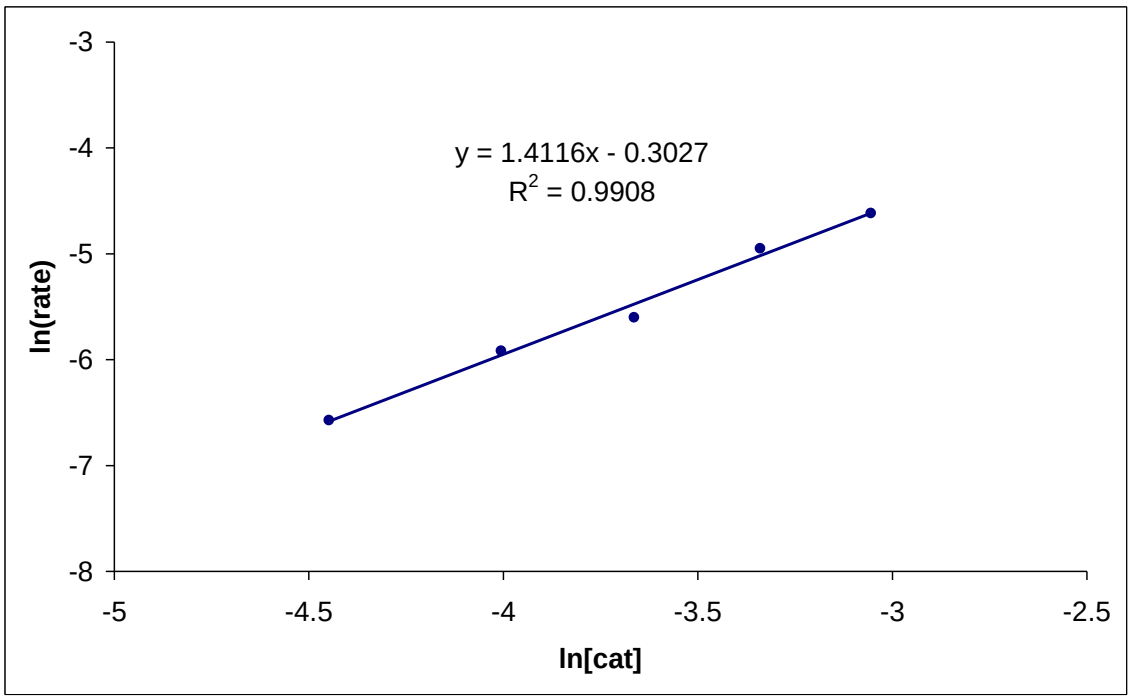

Figure S6. van't Hoff plot for the hydroamination/cyclization of $H_2NCH_2CMe_2(CH_2)_2CH{=}CH_2$ in toluene-d_8 at 90°C using the precatalyst [Cp*Zr$(NMe_2)_2$(PhPhOx)]. The line is the least-squares fit to the data points.

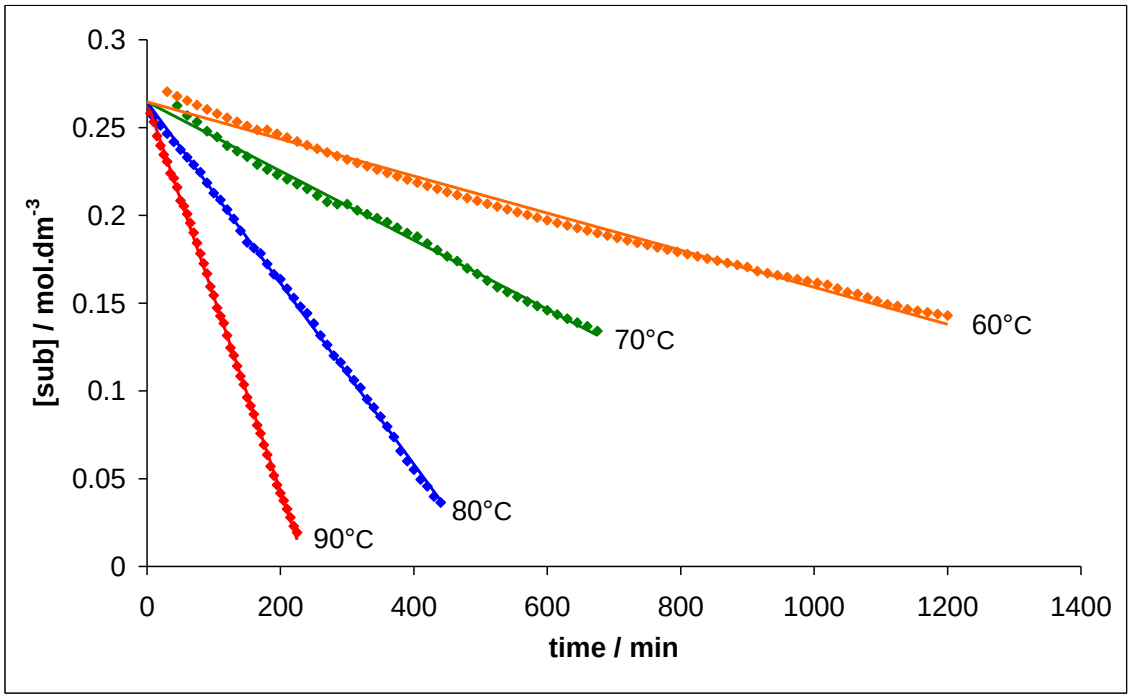

Figure S7. Kinetic plots of [substrate] versus time for hydroamination / cyclization of $H_2NCH_2CPh_2CH_2CH{=}CH_2$ as a function of temperature using [Cp*Zr$(NMe_2)_2$(PhPhOx)] precatalyst in toluene-d_8. The lines are least-squares fits to the data points.

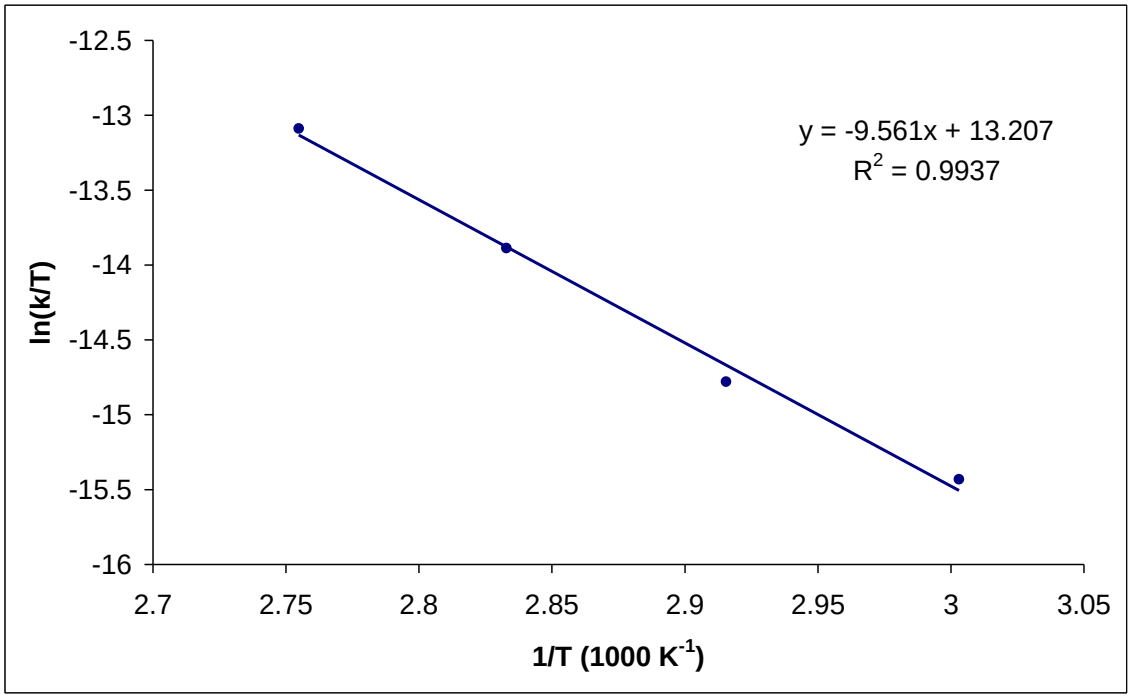

Figure S8. Eyring plot for the hydroamination / cyclization of $H_2NCH_2CPh_2CH_2CH{=}CH_2$ using $[Cp^*Zr(NMe_2)_2(PhPhOx)]$ precatalyst in toluene-d_8. The line is the least-squares fit to the data points.

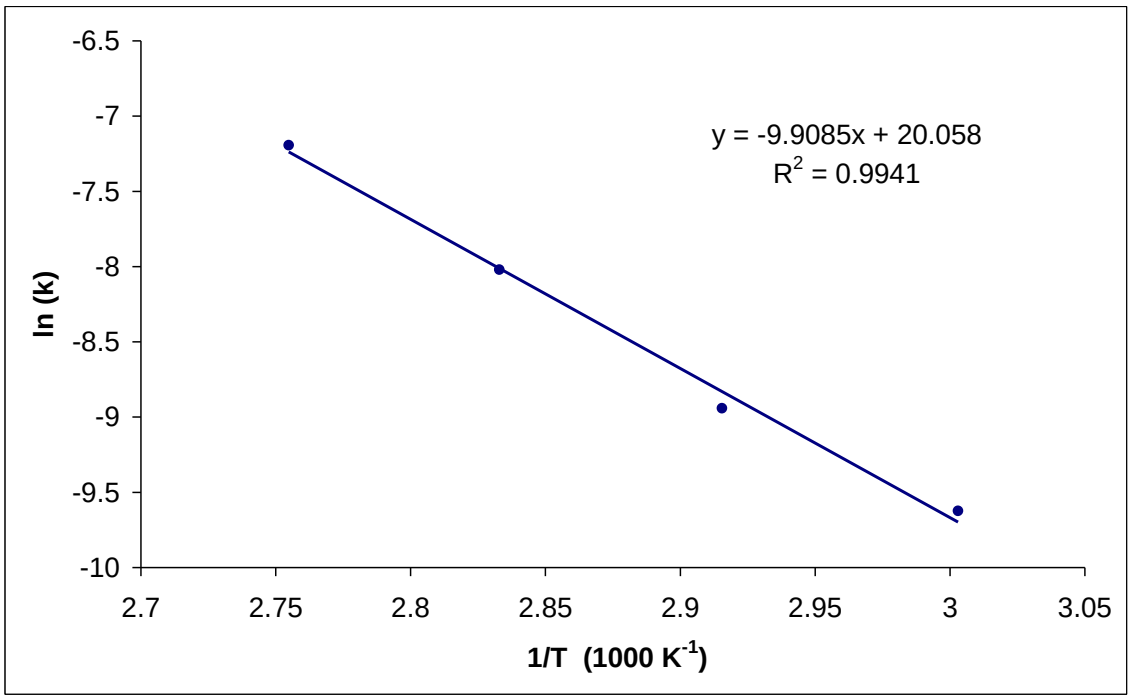

Figure S9. Arrhenius plot for the hydroamination / cyclization of $H_2NCH_2CPh_2CH_2CH{=}CH_2$ using $[Cp^*Zr(NMe_2)_2(PhPhOx)]$ precatalyst in toluene-d_8. The line is the least-squares fit to the data points.

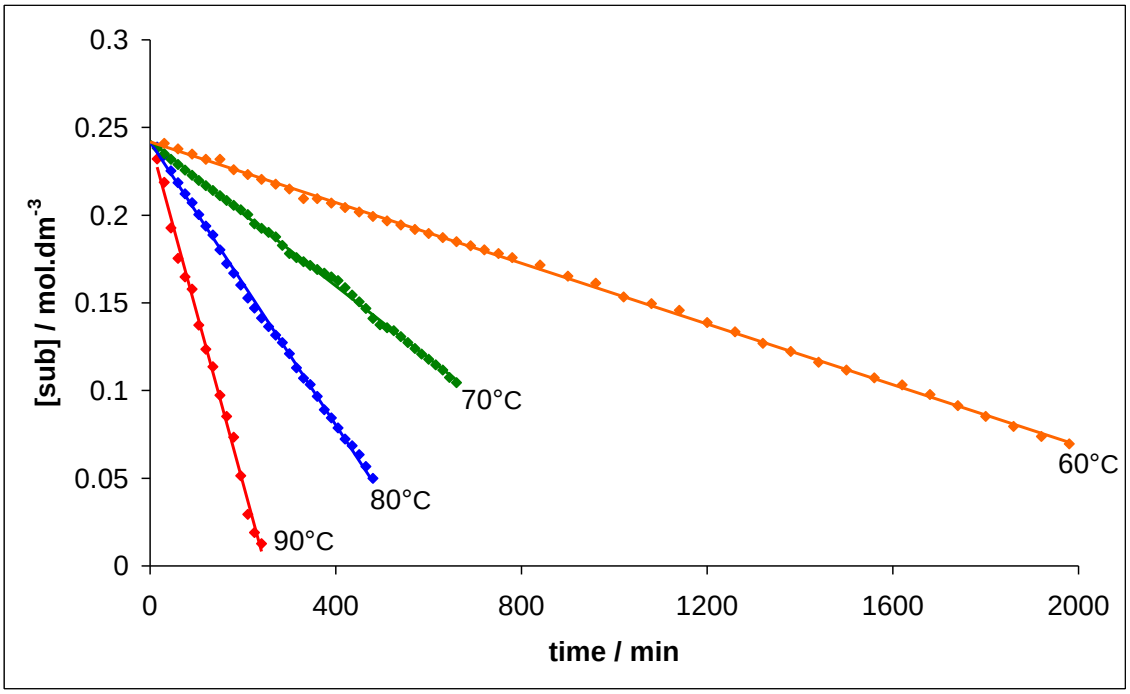

Figure S10. Kinetic plots of [substrate] versus time for hydroamination / cyclization of $H_2NCH_2CPh_2(CH_2)_2CH{=}CH_2$ as a function of temperature using $[Cp^*Zr(NMe_2)_2(PhPhOx)]$ precatalyst in toluene-d_8. The lines are least-squares fits to the data points.

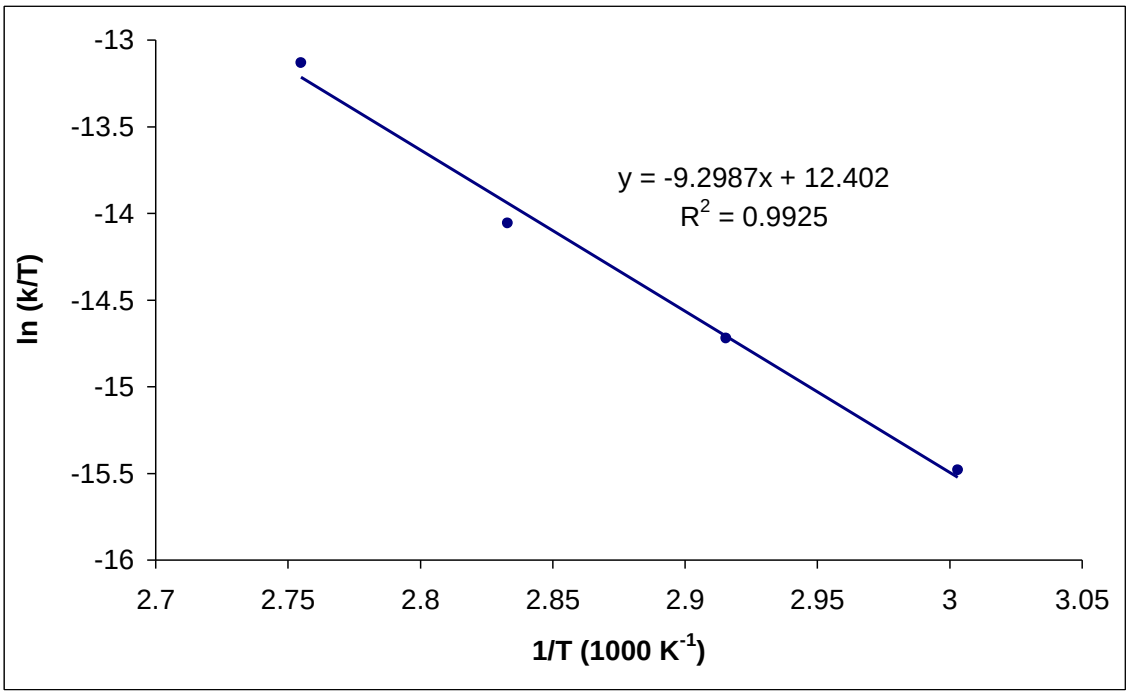

Figure S11. Eyring plot for the hydroamination / cyclization of $H_2NCH_2CPh_2(CH_2)_2CH{=}CH_2$ using $[Cp^*Zr(NMe_2)_2(PhPhOx)]$ precatalyst in toluene-d_8. The line is the least-squares fit to the data points.

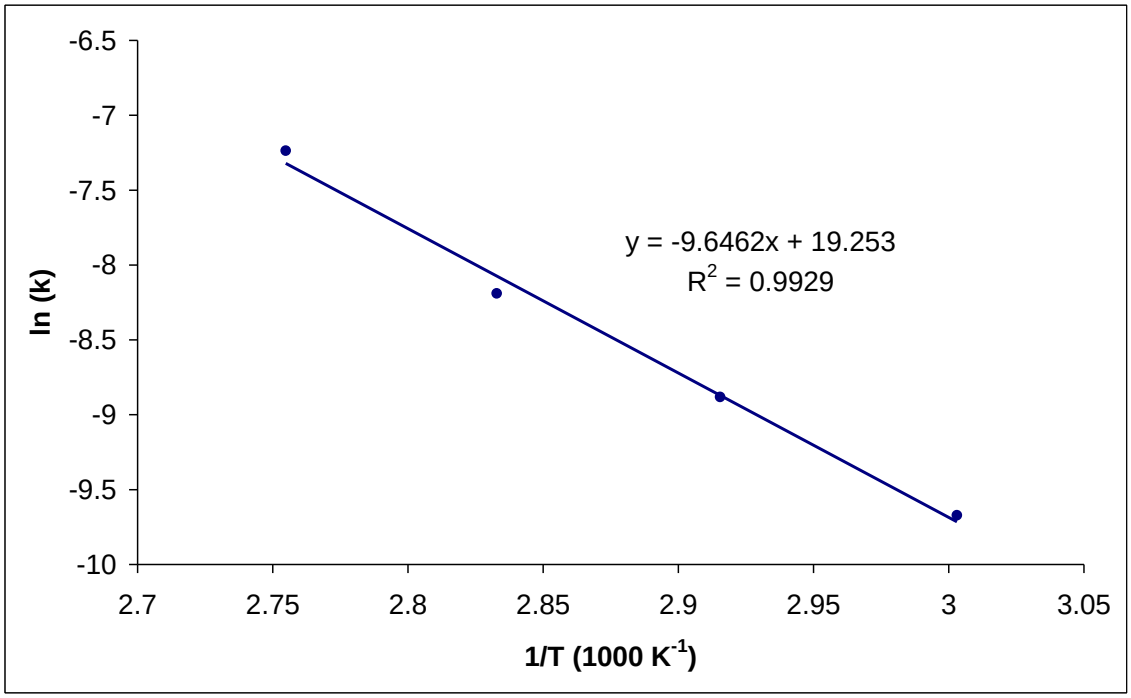

Figure S12. Arrhenius plot for the hydroamination / cyclization of $H_2NCH_2CPh_2(CH_2)_2CH{=}CH_2$ using $[Cp^*Zr(NMe_2)_2(PhPhOx)]$ precatalyst in toluene-d_8. The line is the least-squares fit to the data points.

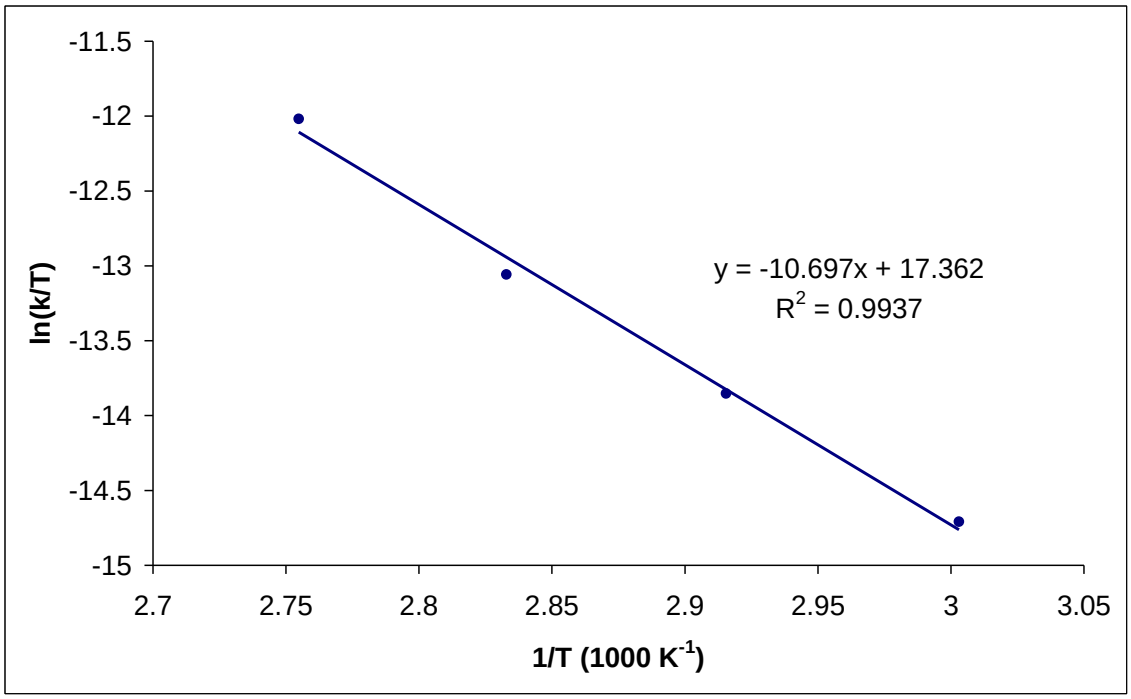

Figure S13. Eyring plot for the hydroamination / cyclization of $H_2NCH_2CMe_2CH_2CH{=}CH_2$ using $[Cp^*Zr(NMe_2)_2(Me_2PhOx)]$ precatalyst in toluene-d_8. The line is the least-squares fit to the data points.

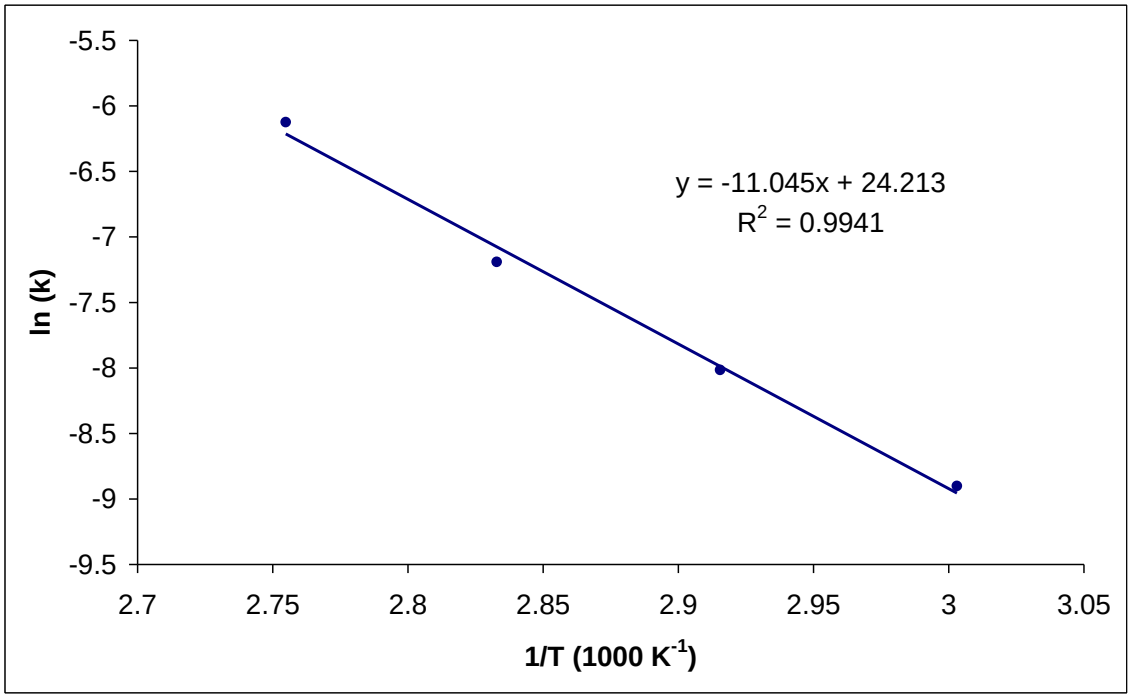

Figure S14. Arrhenius plot for the hydroamination / cyclization of $H_2NCH_2CMe_2CH_2CH{=}CH_2$ using $[Cp^*Zr(NMe_2)_2(Me_2PhOx)]$ precatalyst in toluene-d_8. The line is the least-squares fit to the data points.

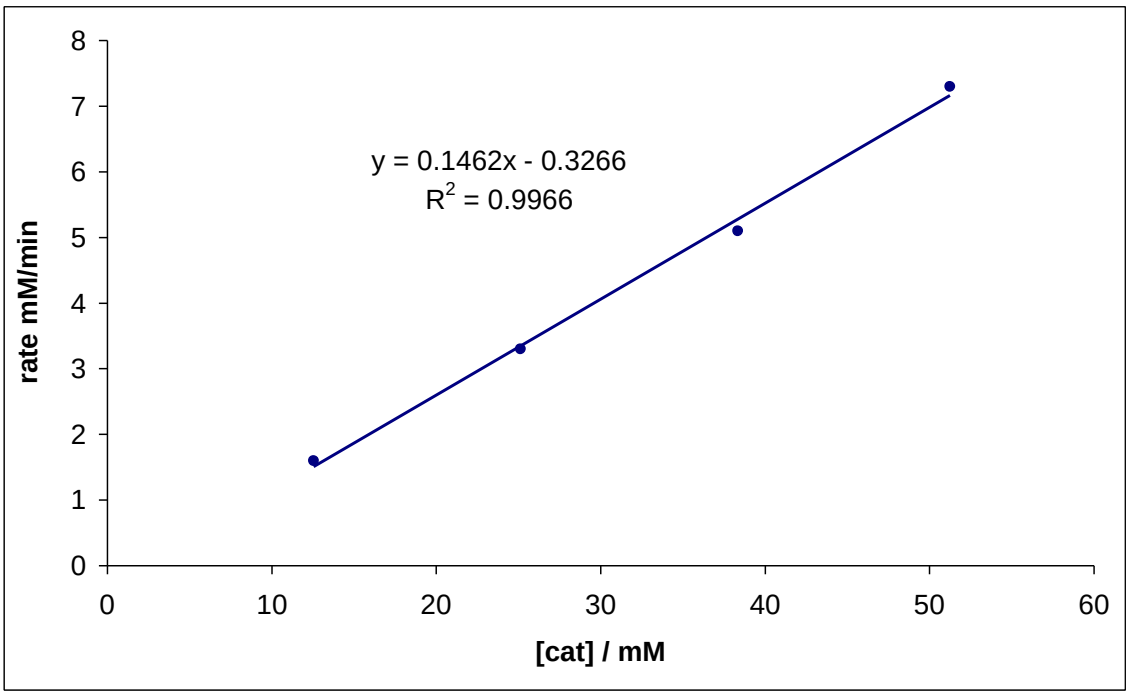

Figure S15. Determination of reaction order in zirconium concentration for the hydroamination/cyclization of $H_2NCH_2CMe_2CH_2CH{=}CH_2$ in toluene-d_8 at 90°C using the precatalyst $[Cp^*Zr(NMe_2)_2(Me_2PhOx)]$. The line is the least-squares fit to the data points.

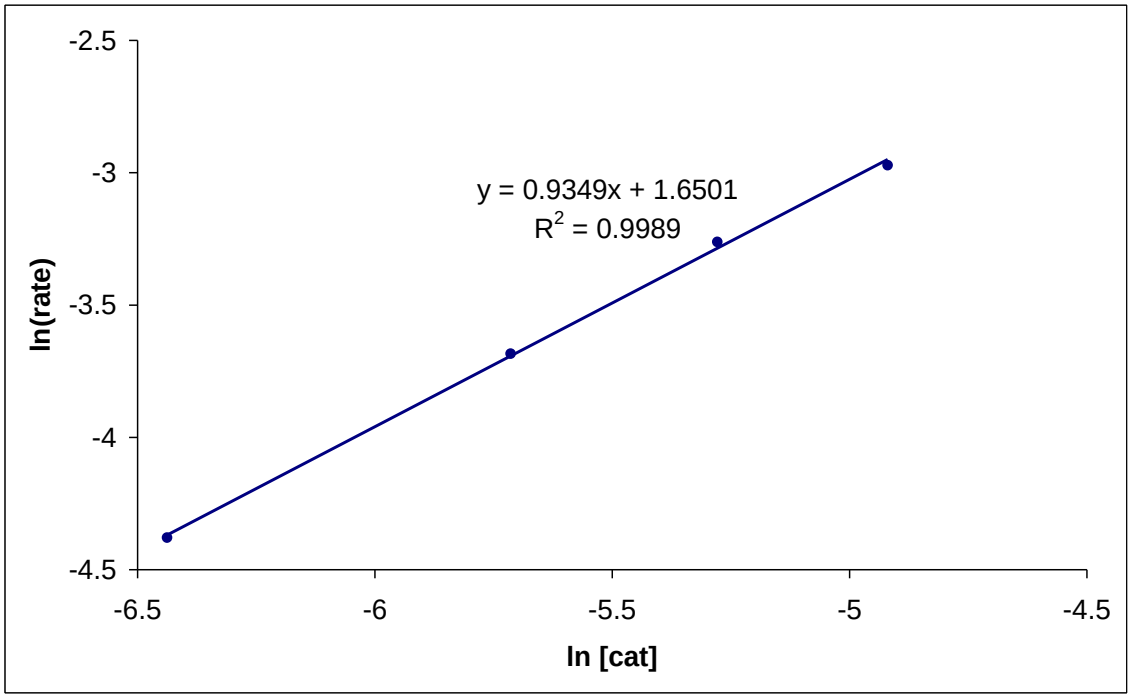

Figure S16. van't Hoff plot for the hydroamination/cyclization of $H_2NCH_2CMe_2CH_2CH{=}CH_2$ in toluene-d_8 at 90°C using the precatalyst $[Cp^*Zr(NMe_2)_2(Me_2PhOx)]$.The line is the least-squares fit to the data points.

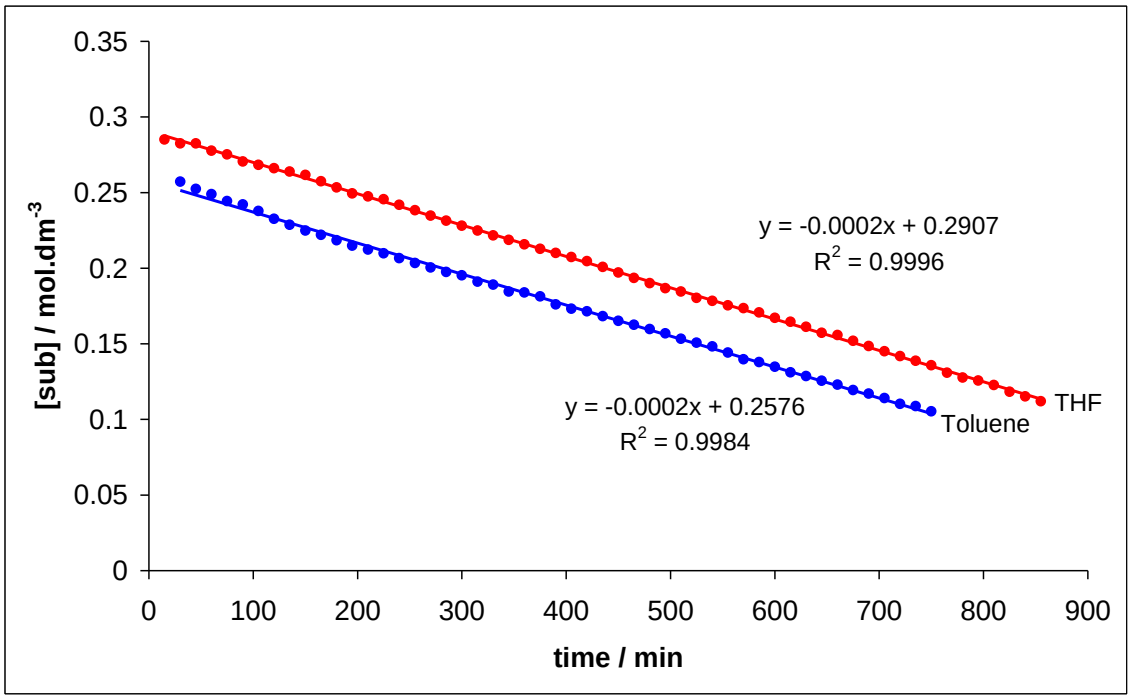

Figure S17. Kinetic plots of [substrate] versus time for hydroamination / cyclization of $H_2NCH_2CMe_2CH_2CH{=}CH_2$ at 60°C, using [Cp*Zr(NMe$_2$)$_2$(Me$_2$PhOx)] precatalyst in toluene-d$_8$ (●) and THF-d$_8$ (●).[cat]$_0$ = 0.025 M. The lines are least-squares fits to the data points.

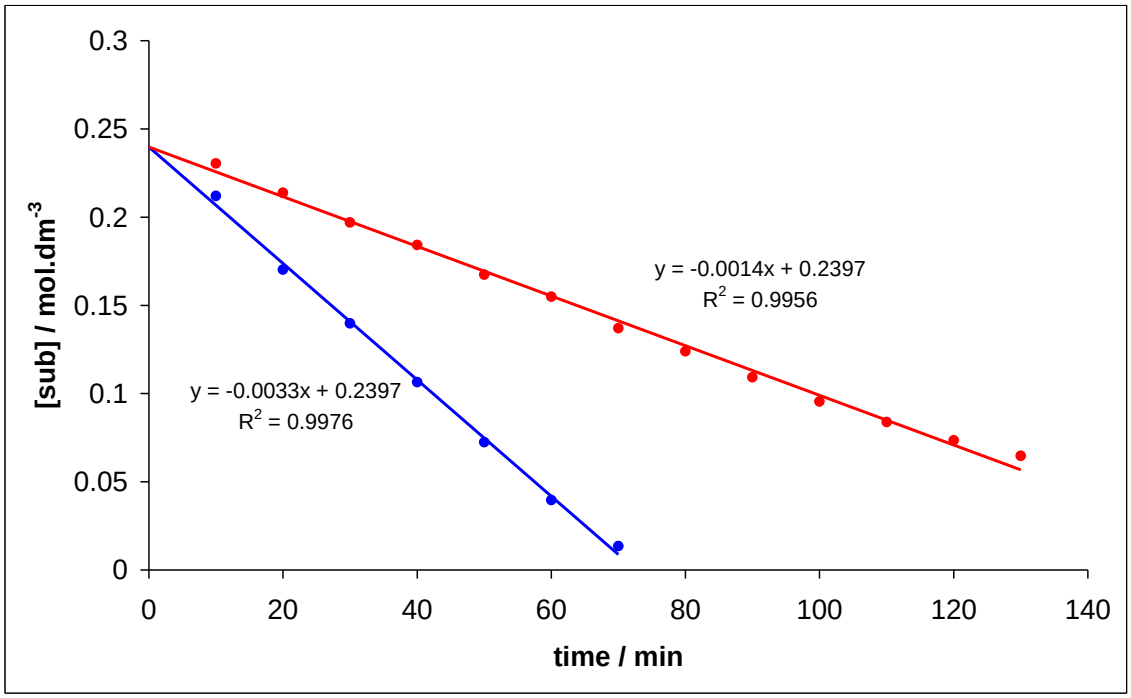

Figure S18. Kinetic plots of [substrate] versus time for hydroamination / cyclization of $H_2NCH_2CMe_2CH_2CH{=}CH_2$ (●) and $D_2NCH_2CMe_2CH_2CH{=}CH_2$ (●) at 90°C, using [Cp*Zr(NMe$_2$)$_2$(Me$_2$PhOx)] precatalyst in toluene-d$_8$. The lines are least-squares fits to the data points.

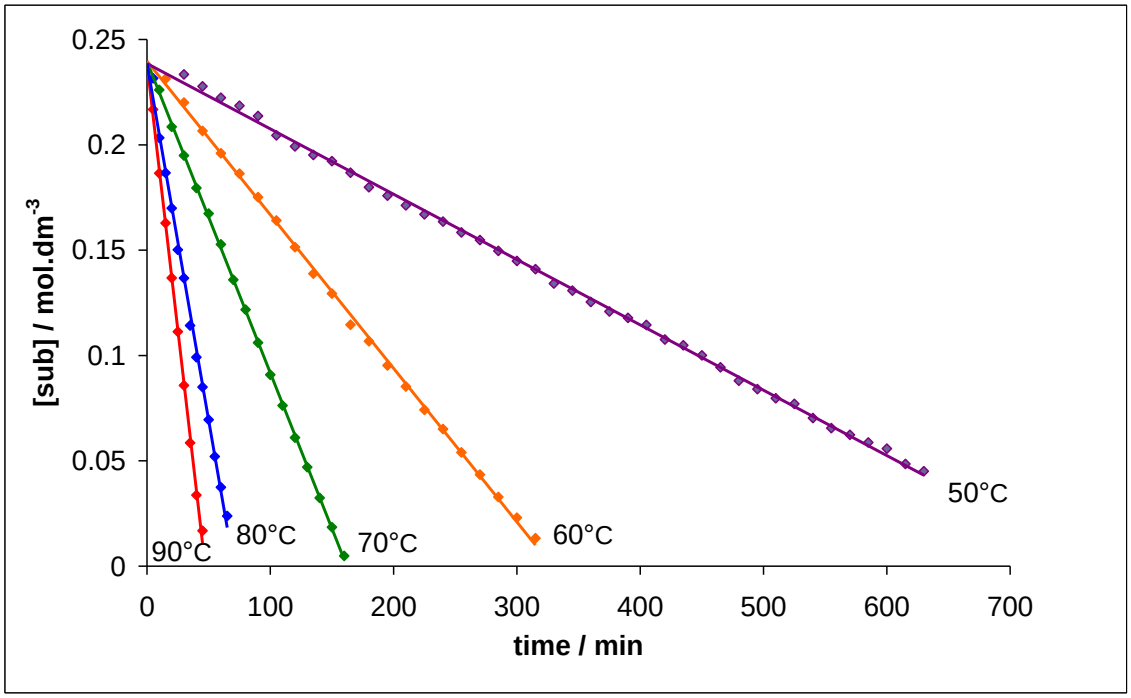

Figure S19. Kinetic plots of [substrate] versus time for hydroamination / cyclization of $H_2NCH_2CMe_2(CH_2)_2CH{=}CH_2$ as a function of temperature using $[Cp^*Zr(NMe_2)_2(Me_2PhOx)]$ precatalyst in toluene-d_8. The lines are least-squares fits to the data points.

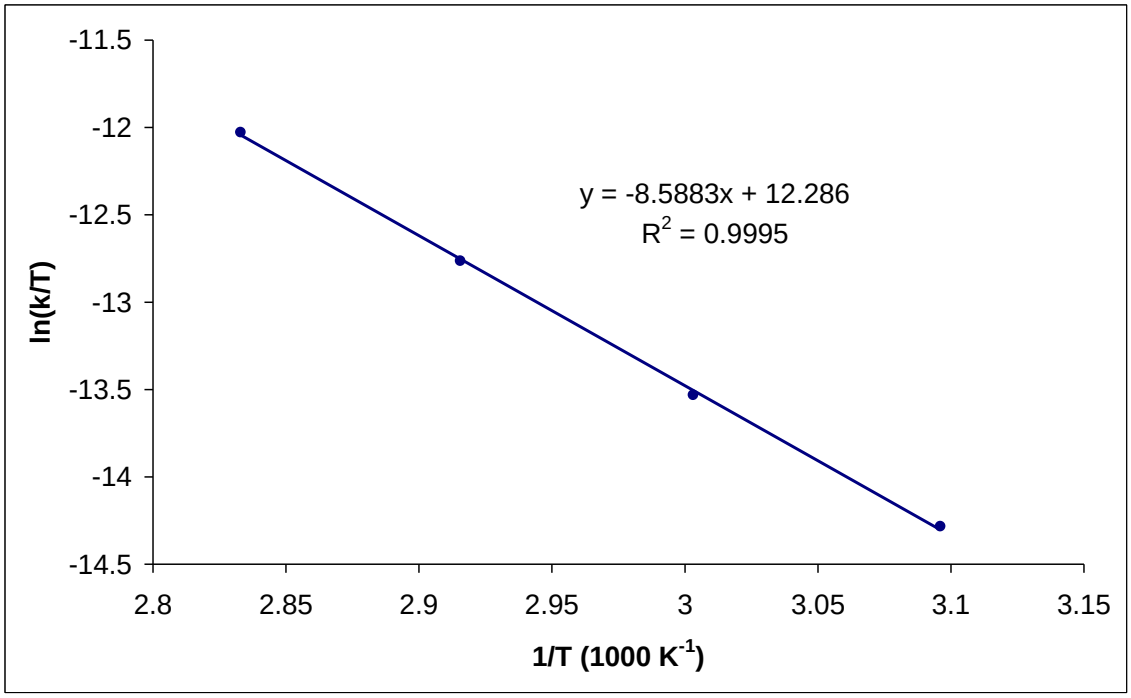

Figure S20. Eyring plot for the hydroamination / cyclization of $H_2NCH_2CMe_2(CH_2)_2CH{=}CH_2$ using $[Cp^*Zr(NMe_2)_2(Me_2PhOx)]$ precatalyst in toluene-d_8. The line is the least-squares fit to the data points.

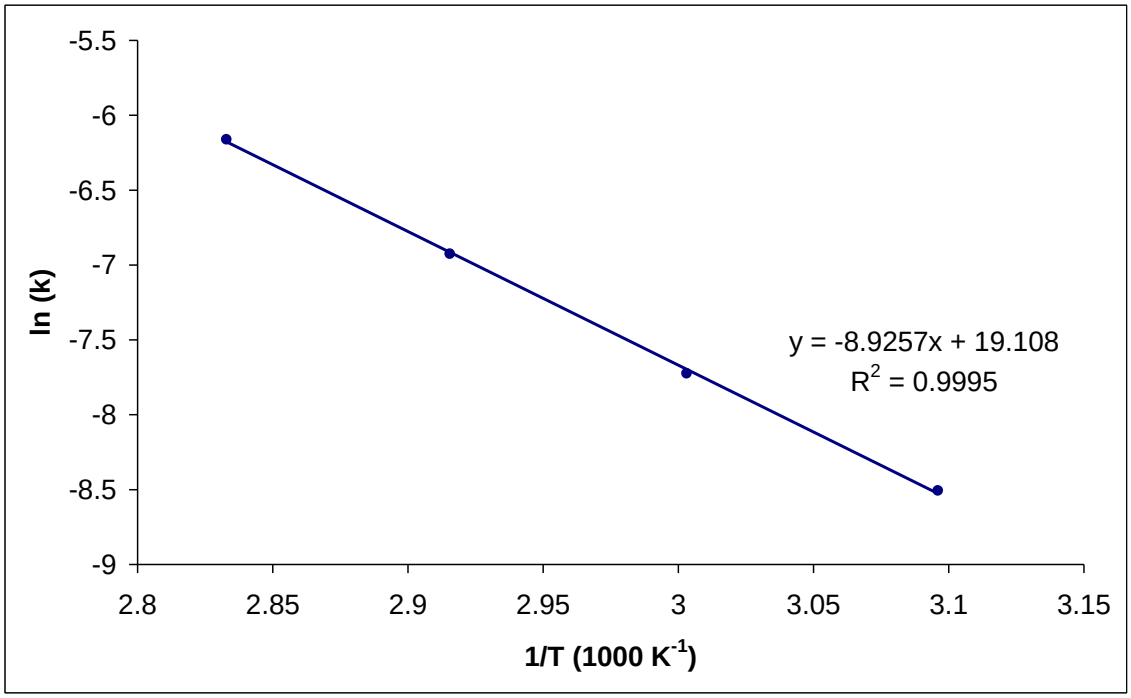

Figure S21. Arrhenius plot for the hydroamination / cyclization of $H_2NCH_2CMe_2(CH_2)_2CH{=}CH_2$ using $[Cp^*Zr(NMe_2)_2(Me_2PhOx)]$ precatalyst in toluene-d_8. The line is the least-squares fit to the data points.

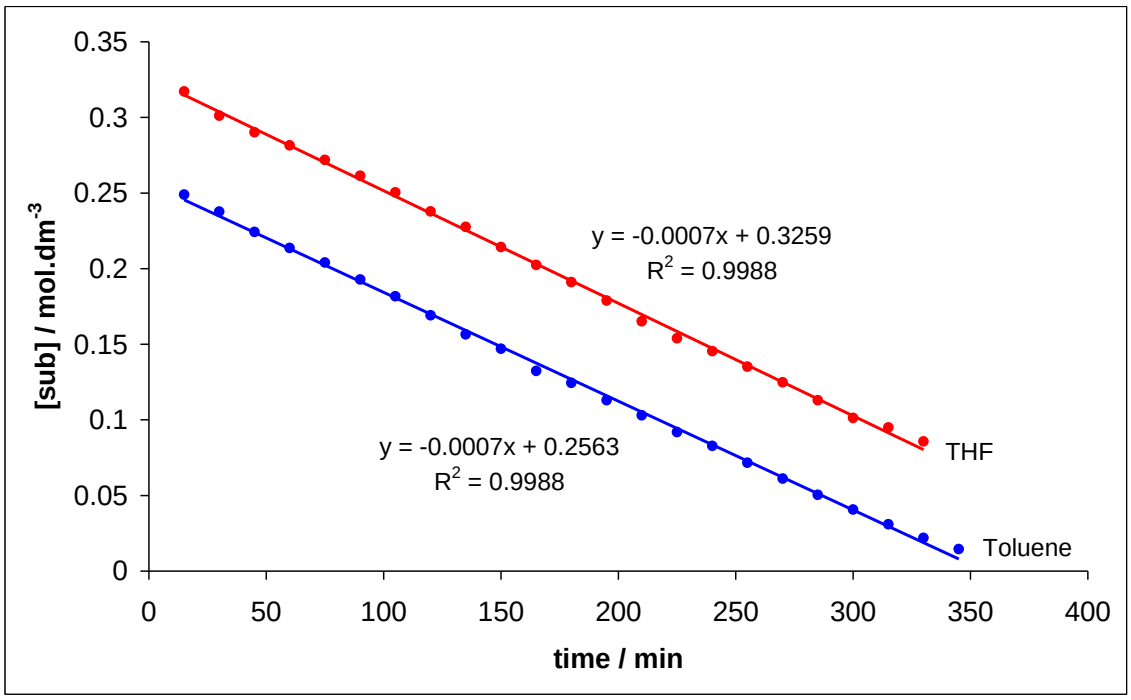

Figure S22. Kinetic plots of [substrate] versus time for hydroamination / cyclization of $H_2NCH_2CMe_2(CH_2)_2CH{=}CH_2$ at 60°C, using $[Cp^*Zr(NMe_2)_2(Me_2PhOx)]$ precatalyst in toluene-d_8 (●) and THF-d_8 (●). $[cat]_0$ = 0.026 M. The lines are least-squares fits to the data points.

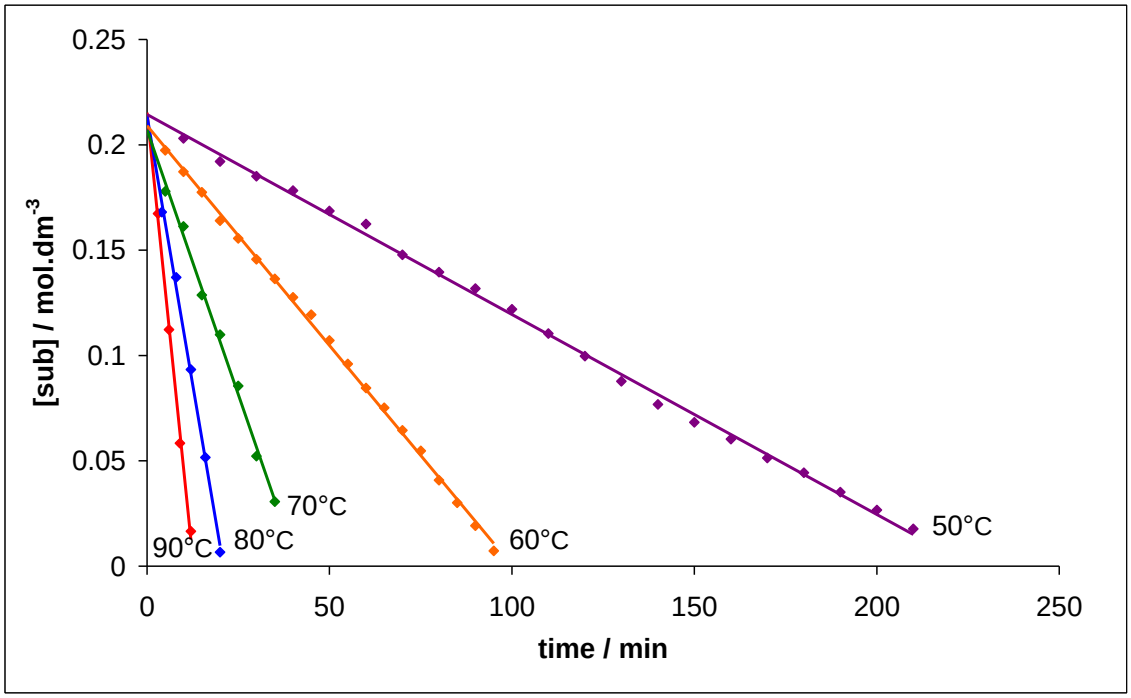

Figure S23. Kinetic plots of [substrate] versus time for hydroamination / cyclization of $H_2NCH_2CPh_2CH_2CH{=}CH_2$ as a function of temperature using $[Cp^*Zr(NMe_2)_2(Me_2PhOx)]$ precatalyst in toluene-d_8. The lines are least-squares fits to the data points.

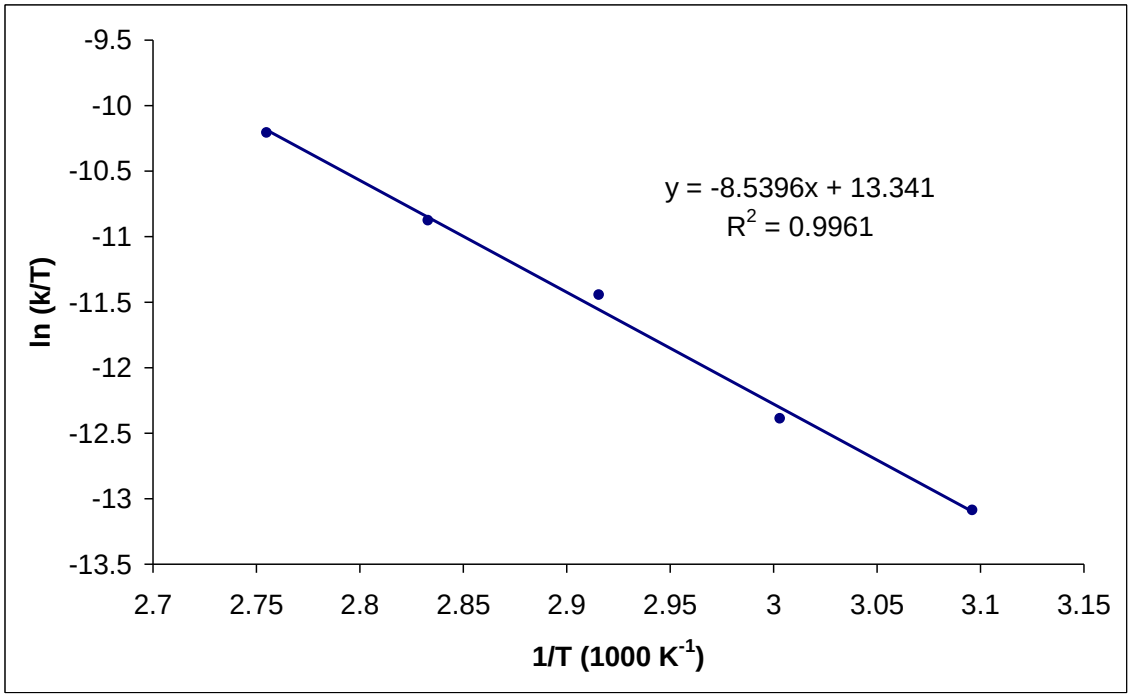

Figure S24. Eyring plot for the hydroamination / cyclization of $H_2NCH_2CPh_2CH_2CH{=}CH_2$ using $[Cp^*Zr(NMe_2)_2(Me_2PhOx)]$ precatalyst in toluene-d_8. The line is the least-squares fit to the data points.

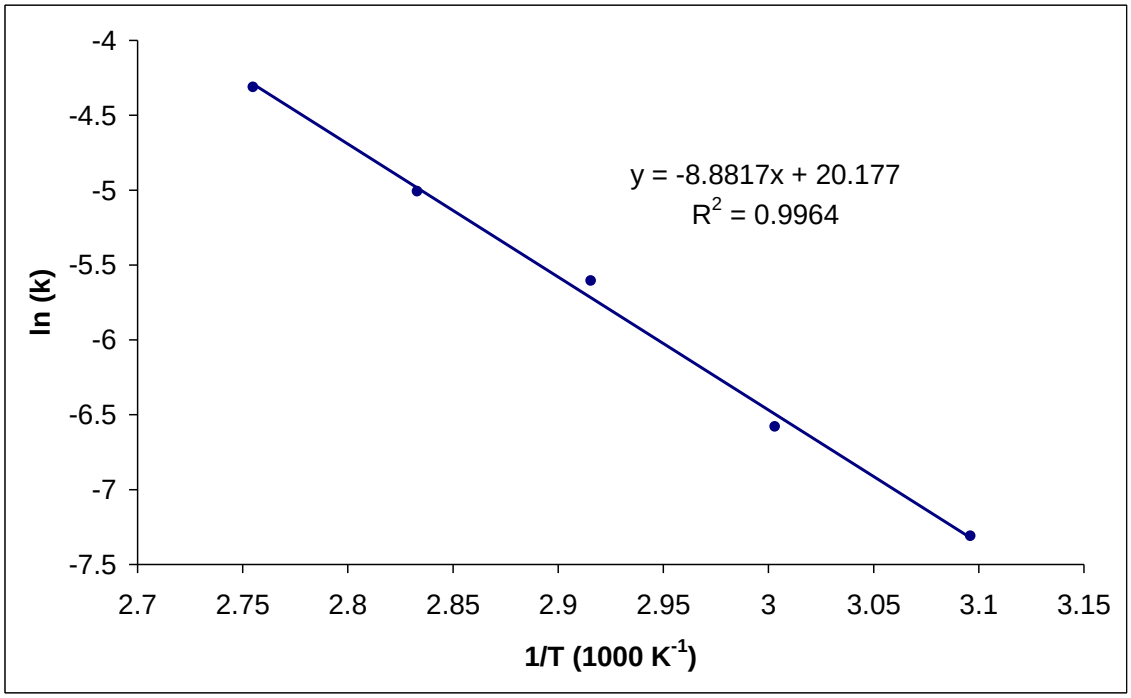

Figure S25. Arrhenius plot for the hydroamination / cyclization of $H_2NCH_2CPh_2CH_2CH{=}CH_2$ using $[Cp^*Zr(NMe_2)_2(Me_2PhOx)]$ precatalyst in toluene-d_8. The line is the least-squares fit to the data points.

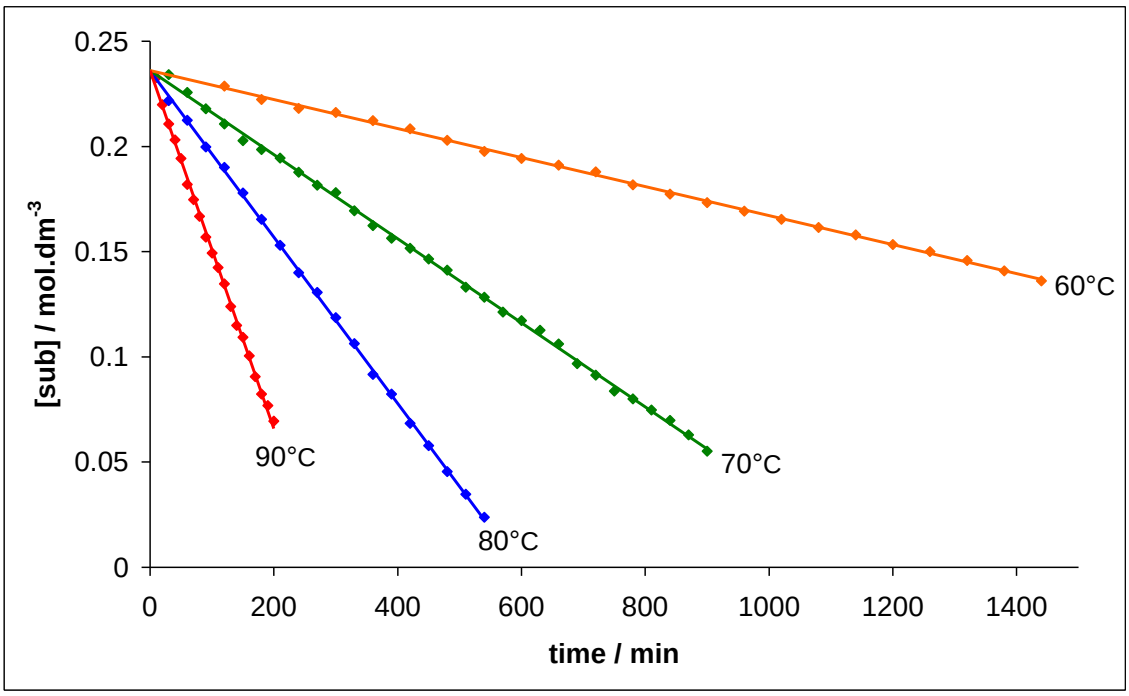

Figure S26. Kinetic plots of [substrate] versus time for hydroamination / cyclization of $H_2NCH_2CPh_2(CH_2)_2CH{=}CH_2$ as a function of temperature using $[Cp^*Zr(NMe_2)_2(Me_2PhOx)]$ precatalyst in toluene-d_8. The lines are least-squares fits to the data points.

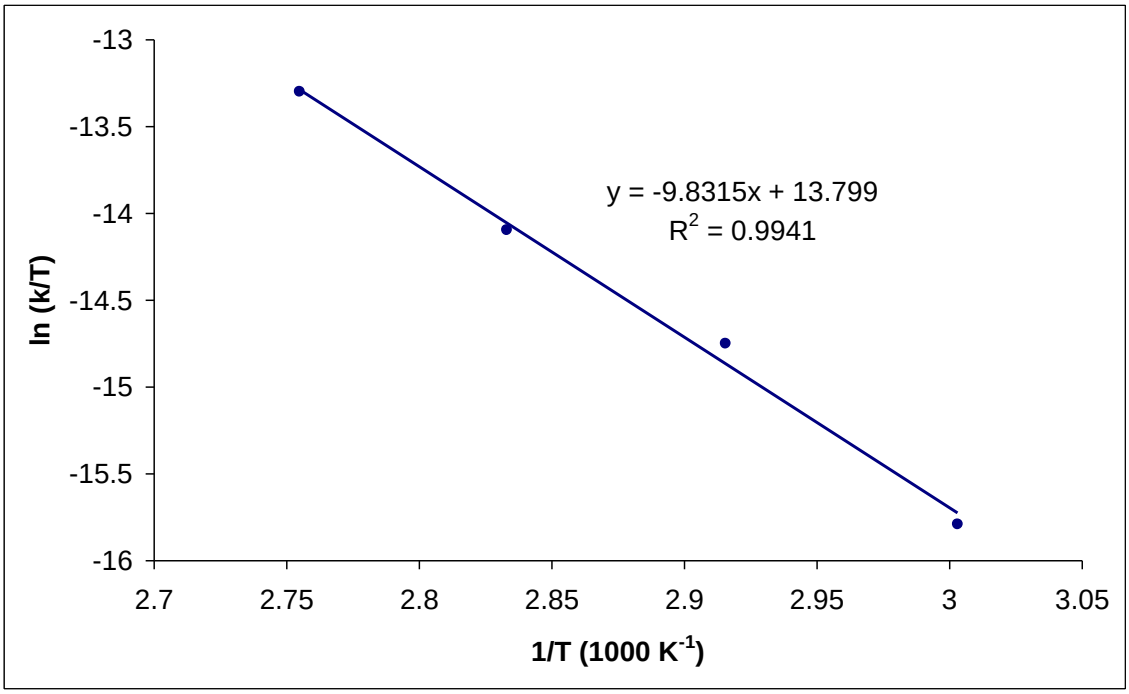

Figure S27. Eyring plot for the hydroamination / cyclization of $H_2NCH_2CPh_2(CH_2)_2CH{=}CH_2$ using $[Cp^*Zr(NMe_2)_2(Me_2PhOx)]$ precatalyst in toluene-d_8. The line is the least-squares fit to the data points.

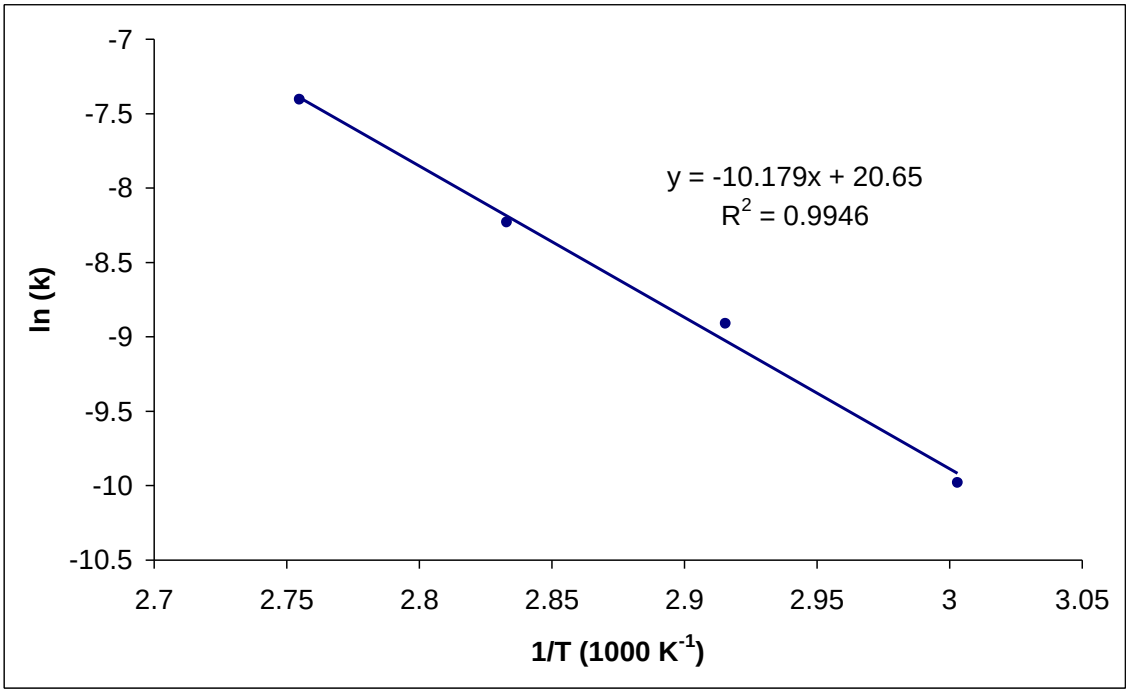

Figure S28. Arrhenius plot for the hydroamination / cyclization of $H_2NCH_2CPh_2(CH_2)_2CH{=}CH_2$ using $[Cp^*Zr(NMe_2)_2(Me_2PhOx)]$ precatalyst in toluene-d_8. The line is the least-squares fit to the data points.

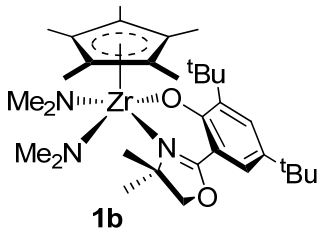
Me2N
Zr
O
tBu
Me2N
N
tBu
O
1b

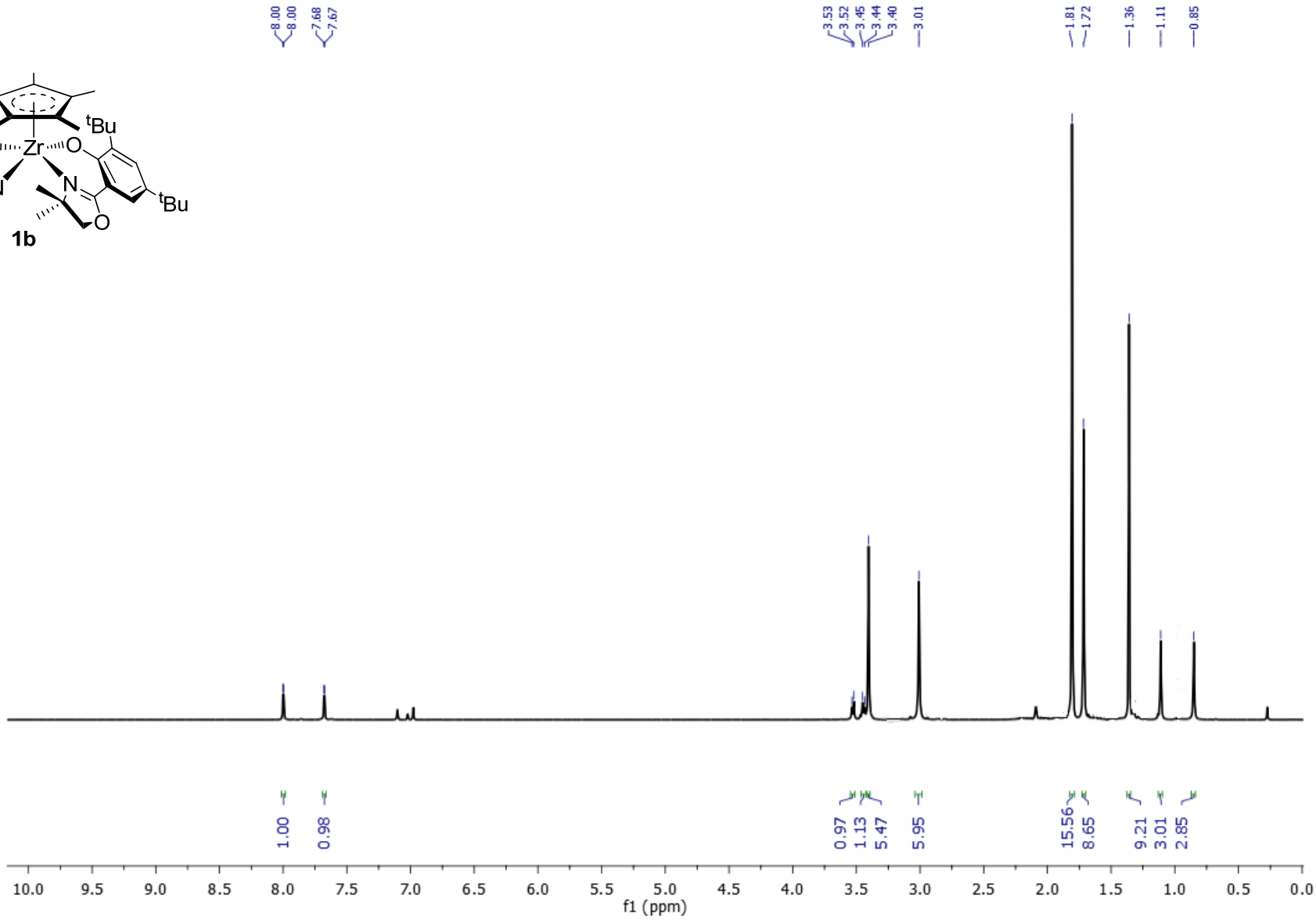
8.00
8.00
7.68
7.67
3.53
3.52
3.45
3.44
3.40
3.01
1.81
1.72
1.36
1.11
0.85
1.00
0.98
0.97
1.13
5.47
5.95
15.56
8.65
9.21
3.01
2.85
10.0
9.5
9.0
8.5
8.0
7.5
7.0
6.5
6.0
5.5
5.0
4.5
4.0
3.5
3.0
2.5
2.0
1.5
1.0
0.5
0.0
f1 (ppm)

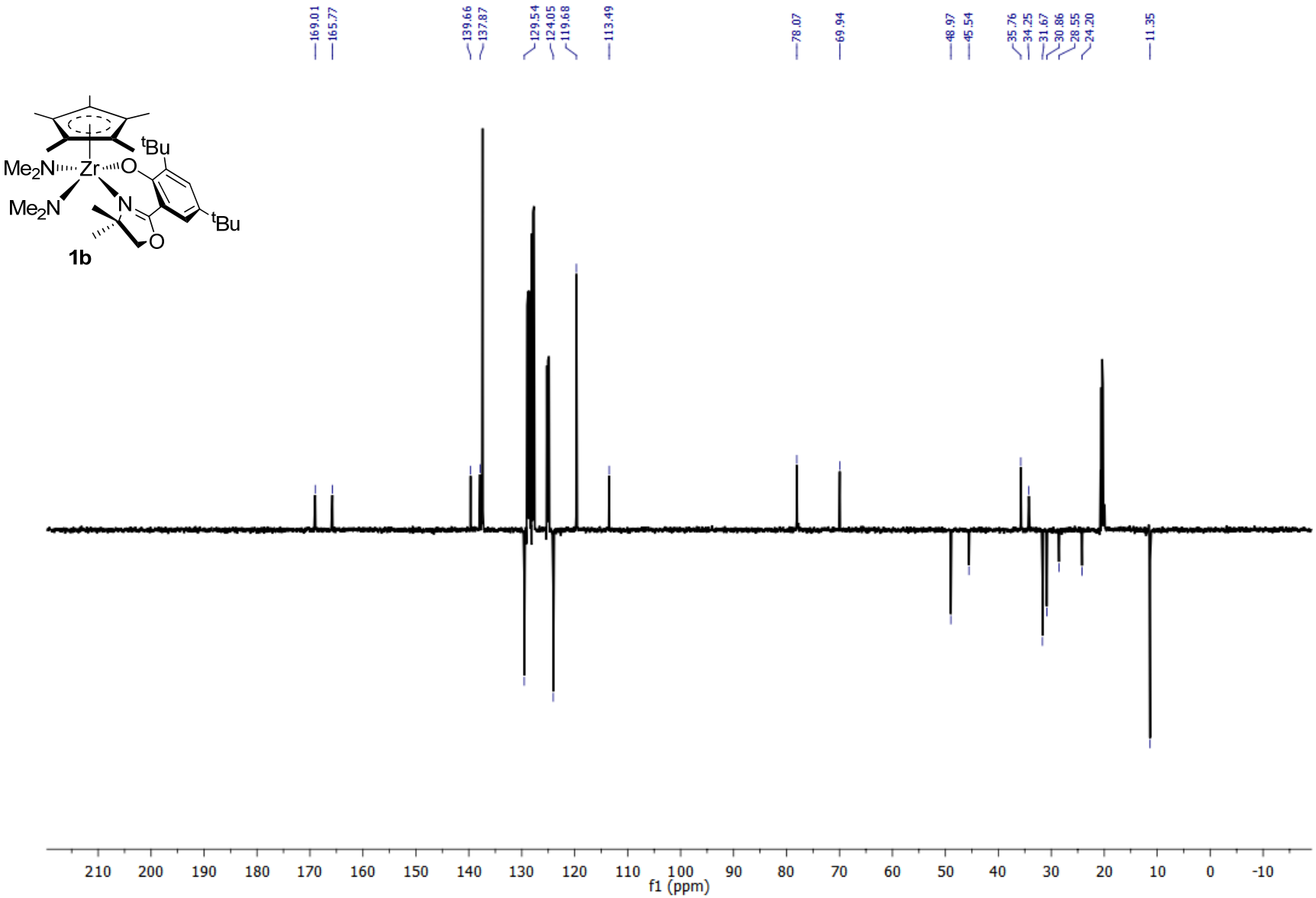
169.01
165.77
139.66
137.87
129.54
124.05
119.68
113.49
78.07
69.94
48.97
45.54
35.76
34.25
31.67
30.86
28.55
24.20
11.35
Me2N
Zr
O
tBu
Me2N
N
tBu
O
1b
210 200 190 180 170 160 150 140 130 120 110 100 90 80 70 60 50 40 30 20 10 0 -10
f1 (ppm)

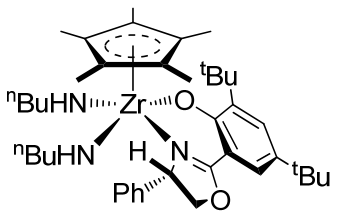
nBuHN
Zr
O
tBu
nBuHN
H
N
tBu
Ph
O

1f

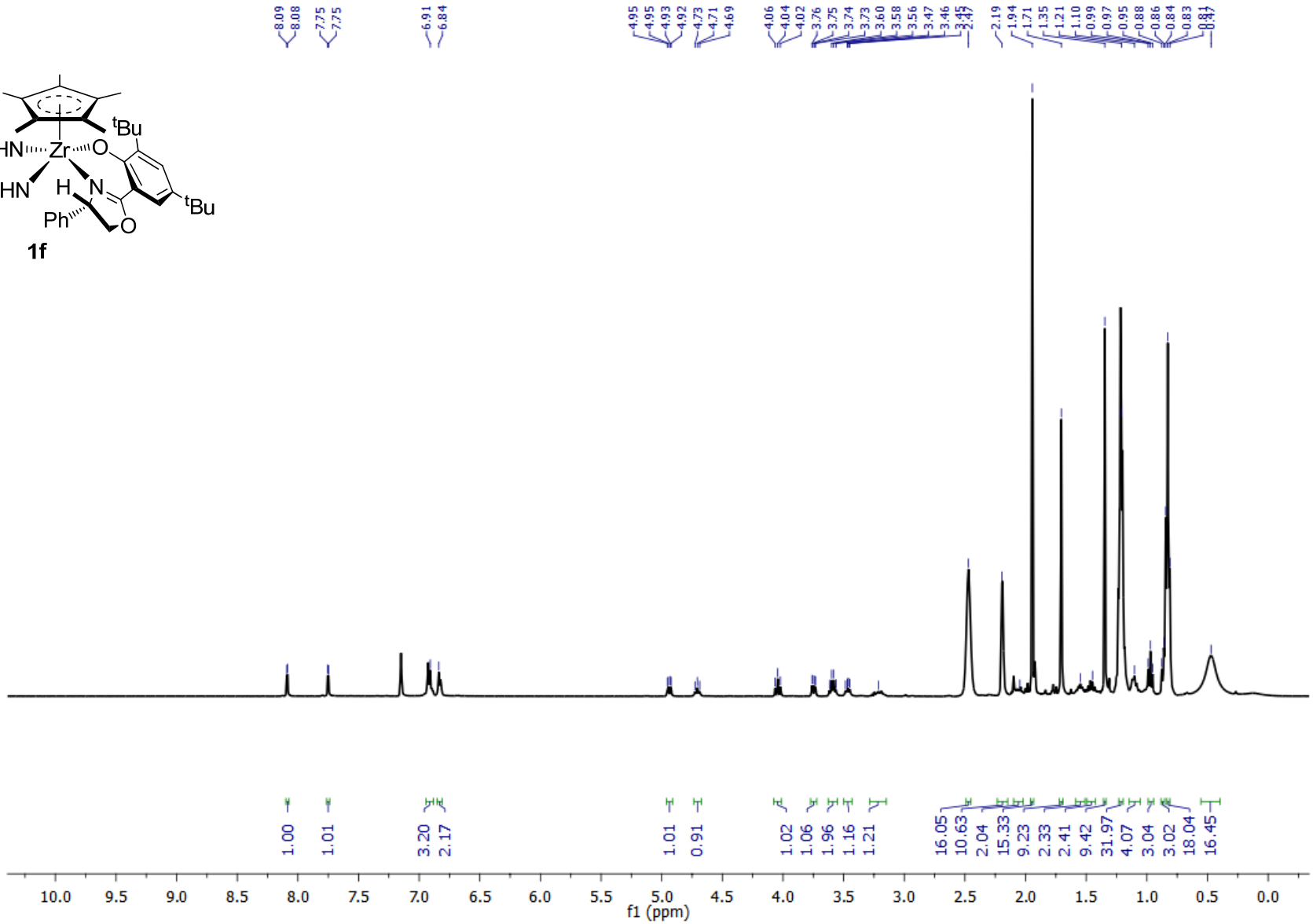
8.09 8.08 7.75 7.75 6.91 6.84 4.95 4.95 4.93 4.92 4.73 4.71 4.69 4.06 4.04 4.02 3.76 3.75 3.74 3.73 3.60 3.58 3.56 3.47 3.46 3.45 2.47 2.19 1.94 1.71 1.35 1.21 1.10 0.99 0.97 0.95 0.88 0.86 0.84 0.83 0.81 0.47
1.00 1.01 3.20 2.17 1.01 0.91 1.02 1.06 1.96 1.16 1.21 16.05 10.63 2.04 15.33 9.23 2.33 2.41 9.42 31.97 4.07 3.04 3.02 18.04 16.45
10.0 9.5 9.0 8.5 8.0 7.5 7.0 6.5 6.0 5.5 5.0 4.5 4.0 3.5 3.0 2.5 2.0 1.5 1.0 0.5 0.0
f1 (ppm)

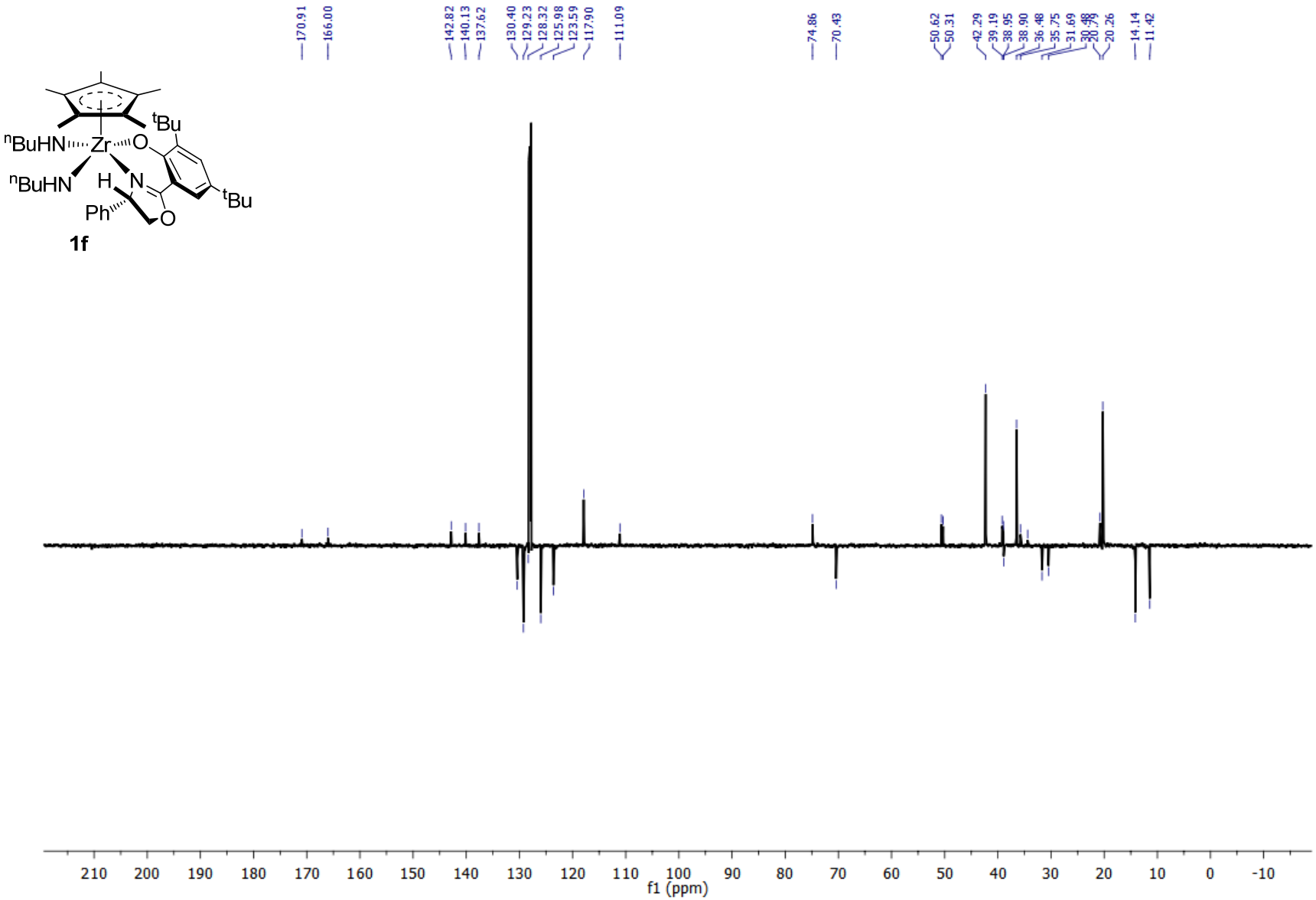
170.91
166.00
142.82
140.13
137.62
130.40
129.23
128.32
125.98
123.59
117.90
111.09
74.86
70.43
50.62
50.31
42.29
39.19
38.95
38.90
36.48
35.75
31.69
20.26
14.14
11.42
nBuHN
Zr
O
tBu
nBuHN
H
N
tBu
Ph
O
1f
210 200 190 180 170 160 150 140 130 120 110 100 90 80 70 60 50 40 30 20 10 0 -10
f1 (ppm)

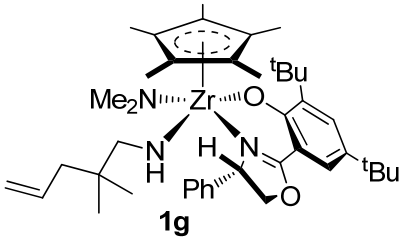
Me2N
Zr
O
tBu
N
H
H
N
Ph
O
tBu

1g

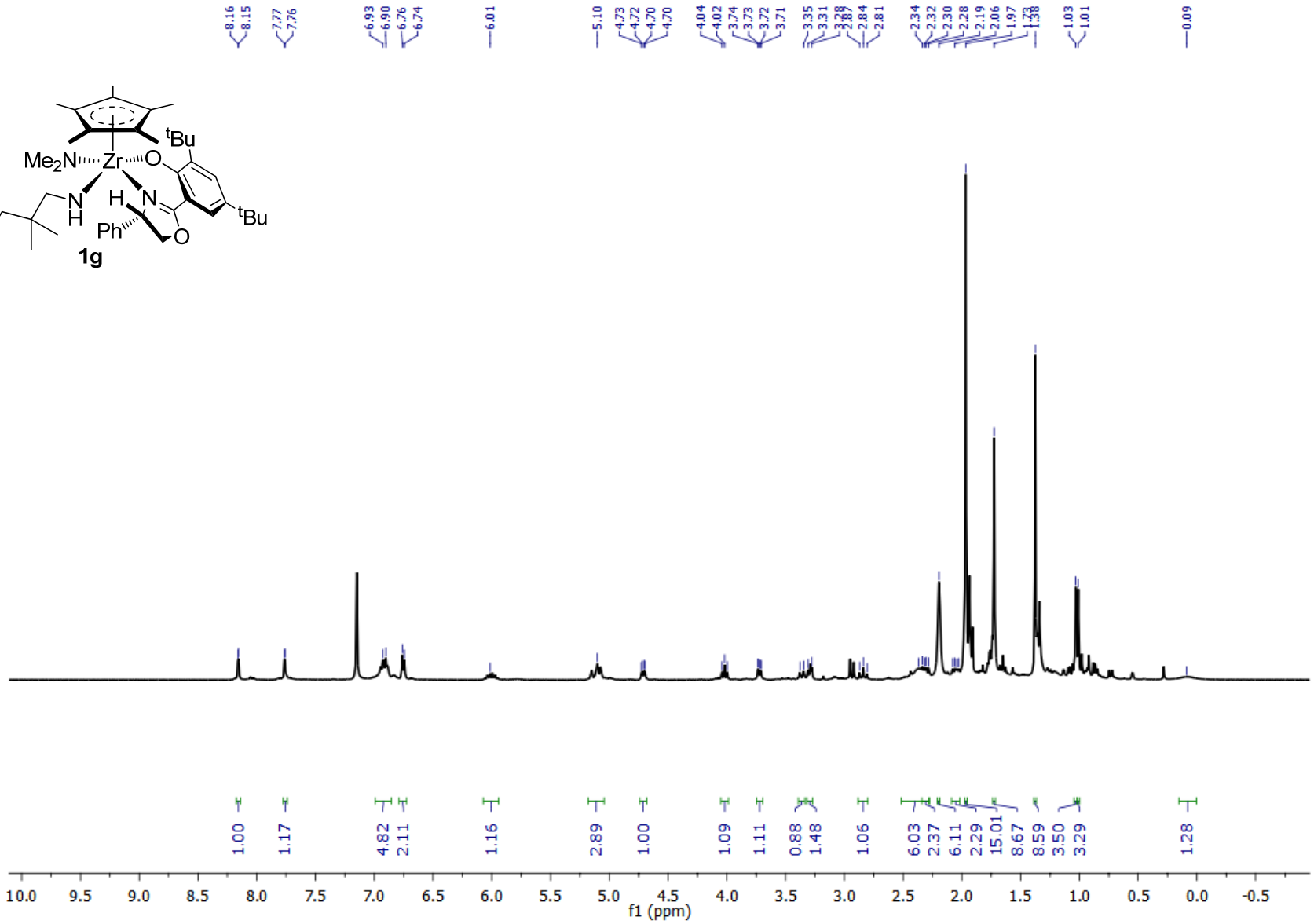
8.16
8.15
7.77
7.76
6.93
6.90
6.76
6.74
6.01
5.10
4.73
4.72
4.70
4.70
4.04
4.02
3.74
3.73
3.72
3.71
3.35
3.31
2.84
2.81
2.34
2.32
2.30
2.28
2.19
2.06
1.97
1.03
1.01
0.09
1.00
1.17
4.82
2.11
1.16
2.89
1.00
1.09
1.11
0.88
1.48
1.06
6.03
2.37
6.11
2.29
15.01
8.67
8.59
3.50
3.29
1.28
10.0
9.5
9.0
8.5
8.0
7.5
7.0
6.5
6.0
5.5
5.0
4.5
4.0
3.5
3.0
2.5
2.0
1.5
1.0
0.5
0.0
-0.5
f1 (ppm)

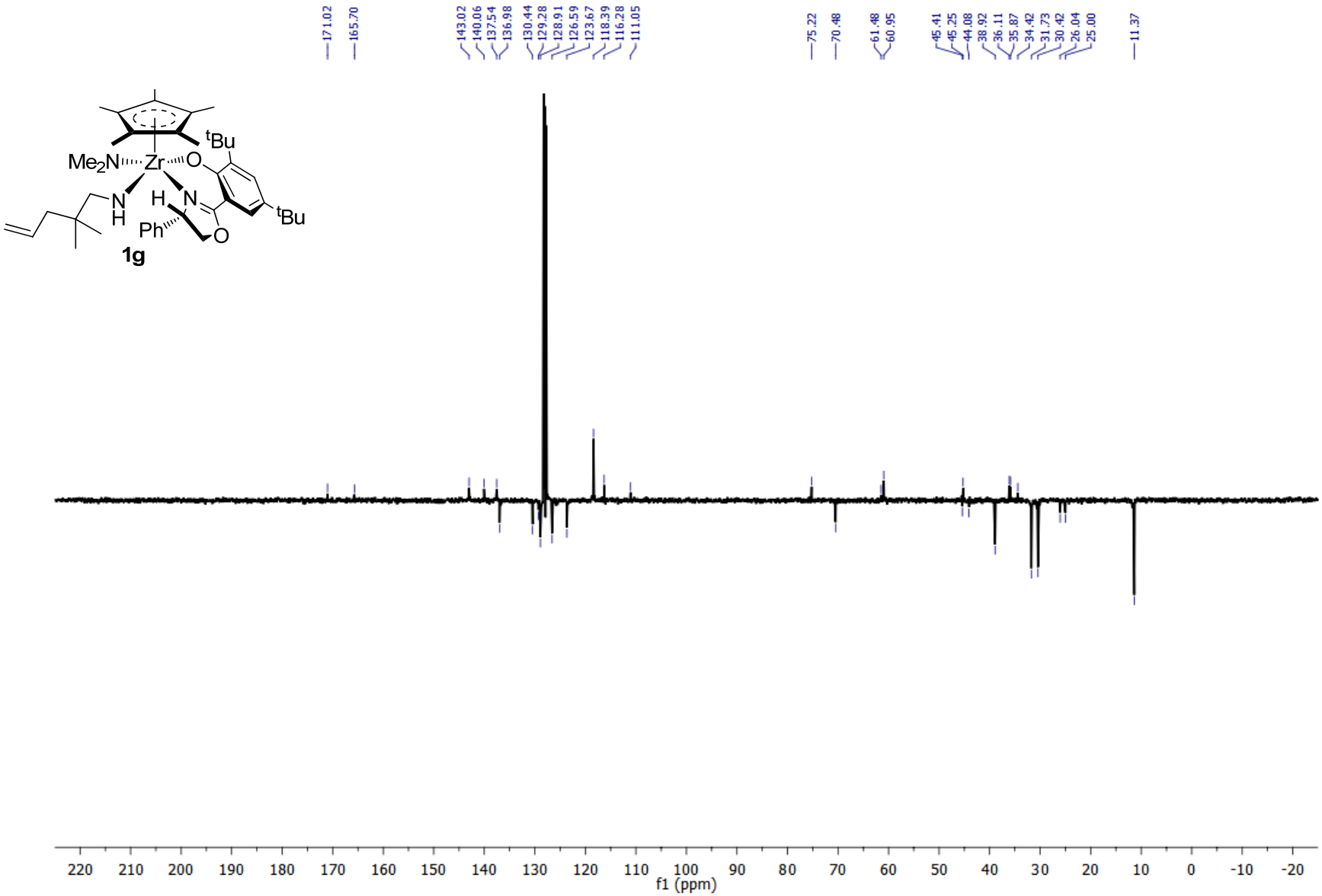
171.02
165.70
143.02
140.06
137.54
136.98
130.44
129.28
128.91
126.59
123.67
118.39
116.28
111.05
75.22
70.48
61.48
60.95
45.41
45.25
44.08
38.92
36.11
35.87
34.42
31.73
30.42
26.04
25.00
11.37
Me2N
Zr
O
tBu
N
H
H
N
Ph
O
tBu
1g
220 210 200 190 180 170 160 150 140 130 120 110 100 90 80 70 60 50 40 30 20 10 0 -10 -20
f1 (ppm)

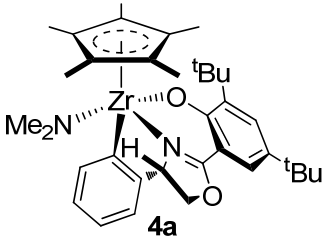
Me2N
Zr
O
tBu
H
N
tBu
O
4a

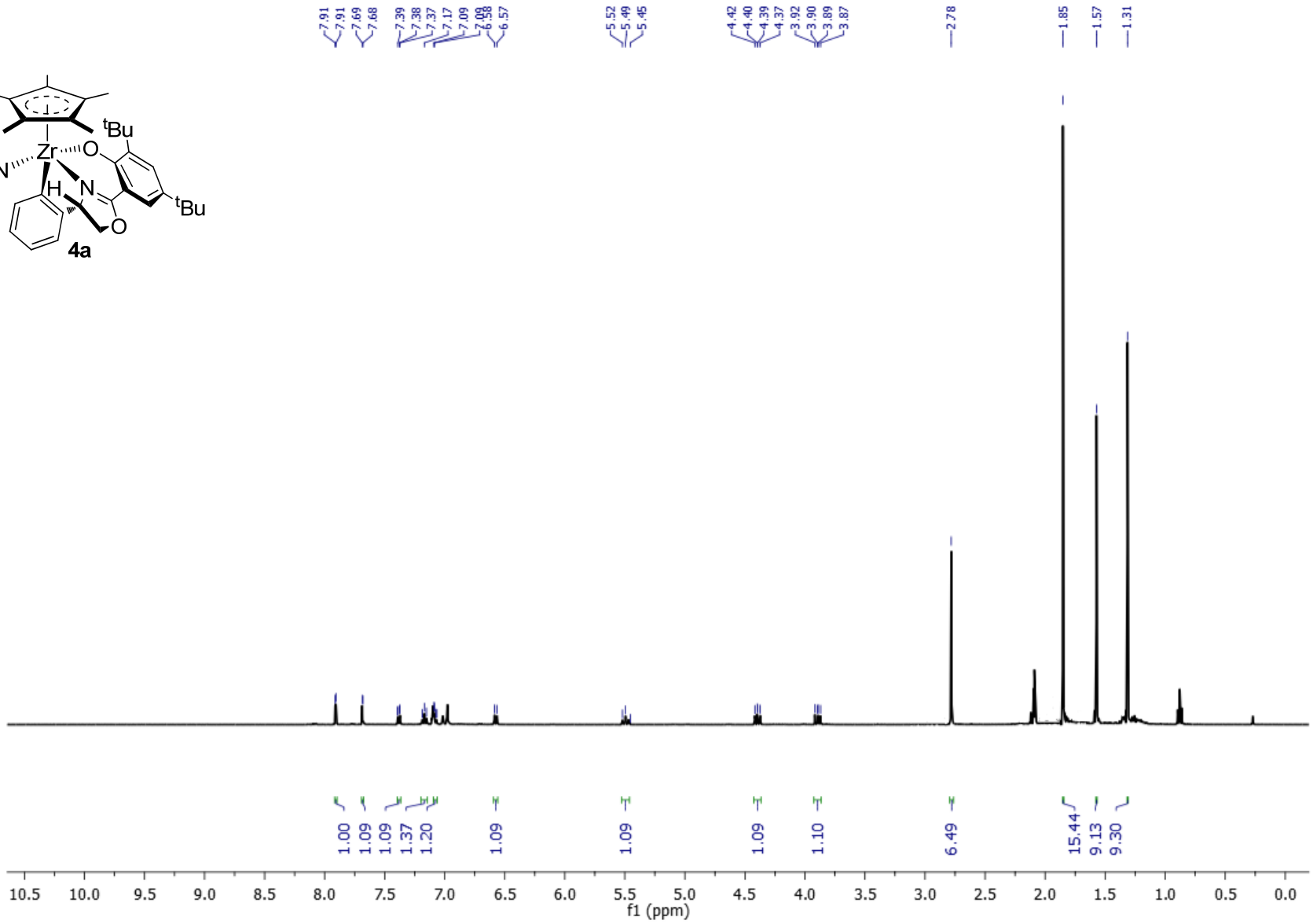
7.91
7.91
7.69
7.68
7.39
7.38
7.37
7.17
7.09
7.09
6.58
6.57
5.52
5.49
5.45
4.42
4.40
4.39
4.37
3.92
3.90
3.89
3.87
2.78
1.85
1.57
1.31
1.00
1.09
1.09
1.37
1.20
1.09
1.09
1.09
1.10
6.49
15.44
9.13
9.30
10.5
10.0
9.5
9.0
8.5
8.0
7.5
7.0
6.5
6.0
5.5
5.0
4.5
4.0
3.5
3.0
2.5
2.0
1.5
1.0
0.5
0.0
f1 (ppm)

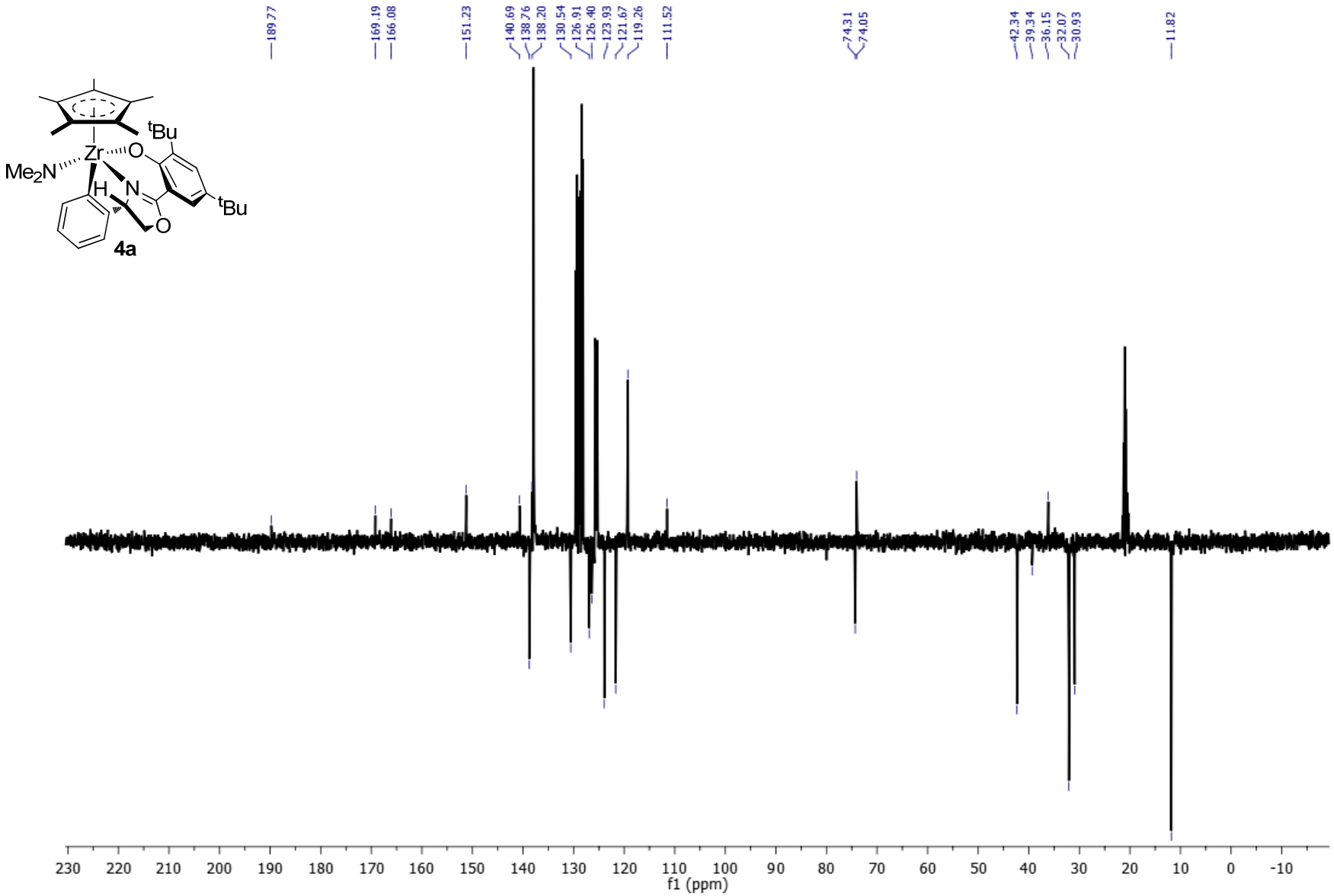
189.77
169.19
166.08
151.23
140.69
138.76
138.20
130.54
126.91
126.40
123.93
121.67
119.26
111.52
74.31
74.05
42.34
39.34
36.15
32.07
30.93
11.82
Me2N
Zr
O
tBu
H
N
O
tBu
4a
230 220 210 200 190 180 170 160 150 140 130 120 110 100 90 80 70 60 50 40 30 20 10 0 -10
f1 (ppm)

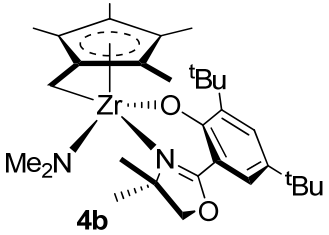

4b

(incomplete reaction: see article text)

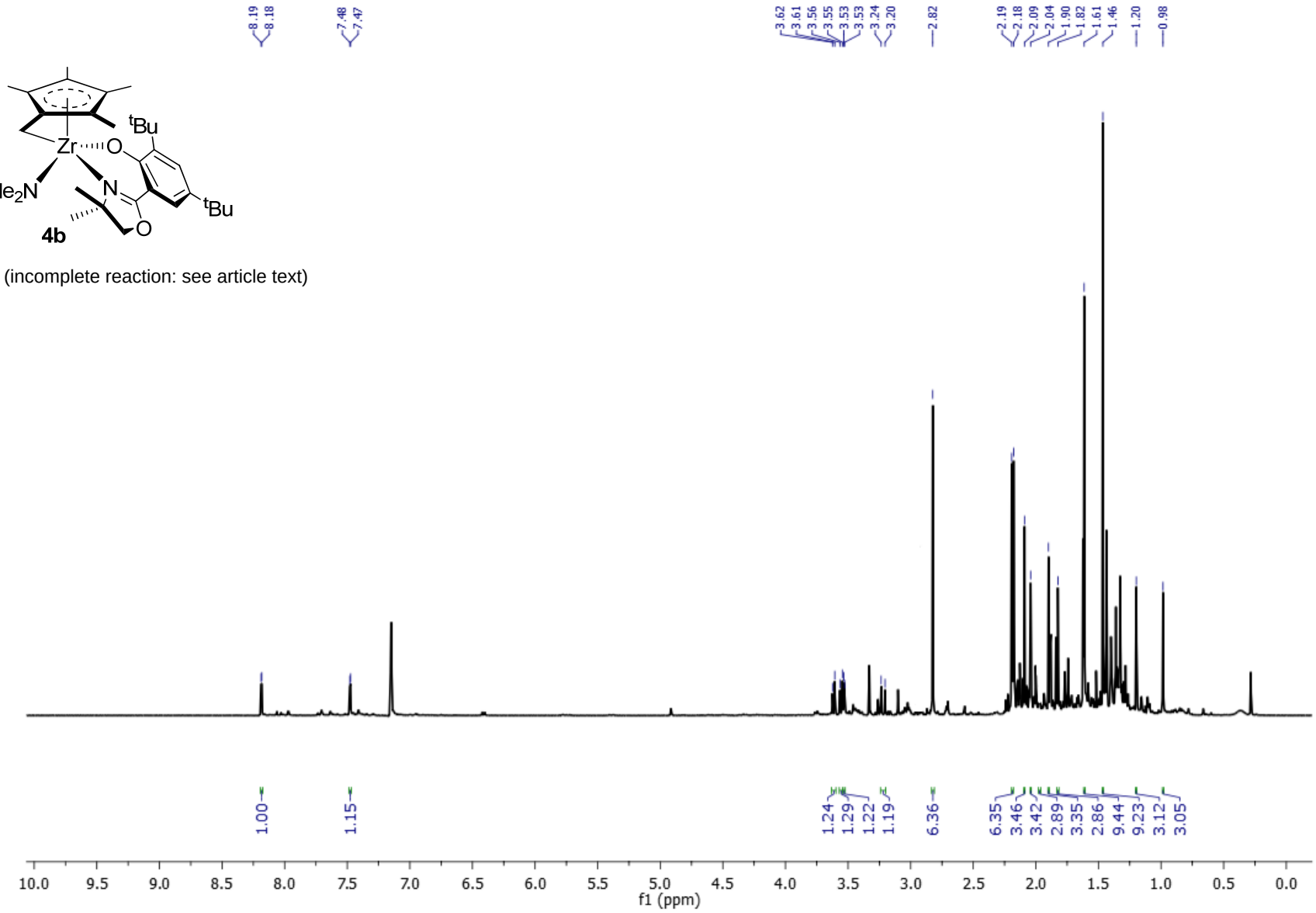

Zr
O
N
O
Me2N
tBu
tBu
4b

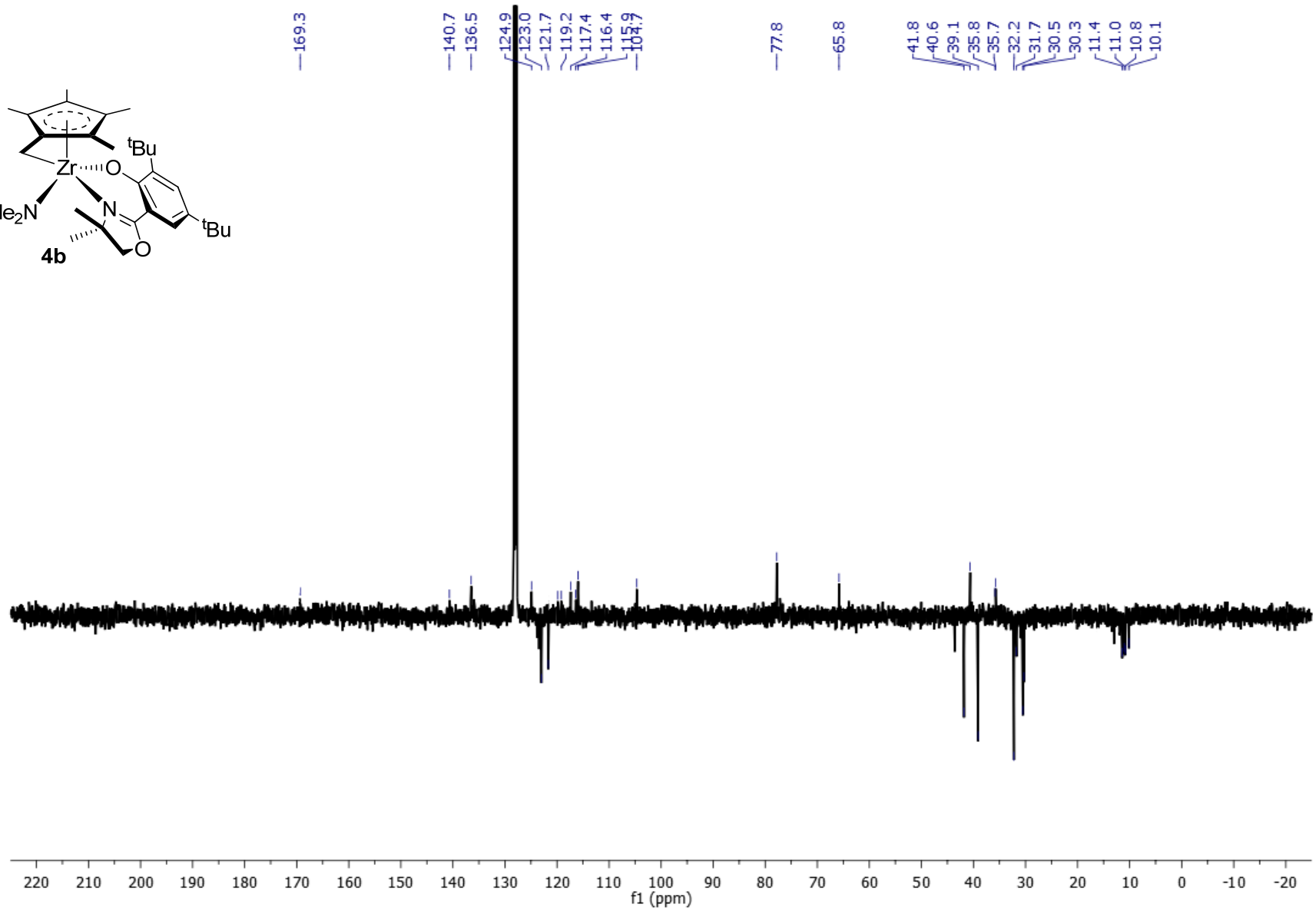
169.3
140.7
136.5
124.9
123.0
121.7
119.2
117.4
116.4
115.9
104.7
77.8
65.8
41.8
40.6
39.1
35.8
35.7
32.2
31.7
30.5
30.3
11.4
11.0
10.8
10.1
220 210 200 190 180 170 160 150 140 130 120 110 100 90 80 70 60 50 40 30 20 10 0 -10 -20
f1 (ppm)